International Journal of Mass Spectrometry 289 (2010) 11–29

Contents lists available at ScienceDirect

International Journal of Mass Spectrometry

journal homepage: www.elsevier.com/locate/ijms

Knudsen effusion mass spectrometric determination of mixing thermodynamic data of liquid Al–Cu–Sn alloy

L. Bencze[a,*], R. Milačič[b], R. Jaćimović[b], D. Žigon[b], L. Mátyás[c], A. Popovič[b]

[a] Eötvös Loránd University, Dept. of Physical Chemistry, H-1117 Budapest, Pázmány Péter sétány 1/A, Hungary
[b] Jozef Stefan Institute, Jamova 39, SLO-1000 Ljubljana, Slovenia
[c] Sapientia University, Department of Technical and Natural Sciences, Libertatii sq. 1, 530104 Miercurea Ciuc, Romania

ARTICLE INFO

Article history:
Received 8 July 2009
Received in revised form
14 September 2009
Accepted 15 September 2009
Available online 24 September 2009

Keywords:
Knudsen effusion mass spectrometry
Redlich–Kister–Muggianu model
Activity
Excess Gibbs energy
Ternary and binary *L*-parameter

ABSTRACT

The vaporisation of a liquid Al–Cu–Sn system has been investigated at 1273–1473 K by Knudsen effusion mass spectrometry (KEMS) and the data fitted to a Redlich–Kister–Muggianu (RKM) sub-regular solution model. Thirty-one different compositions (41 samples) have been examined at eight fixed copper mole fractions, X_{Cu} = 0.10, 0.20, 0.30, 0.333, 0.40, 0.50, 0.60 and 0.70. The ternary *L*-parameters, the thermodynamic activities and the thermodynamic functions of mixing have been evaluated using standard KEMS procedures. In addition, the same quantities were obtained from the measured ion intensity ratios of Al^+ to Cu^+, Al^+ to Sn^+ and Cu^+ to Sn^+ using a mathematical regression technique. The intermediate data obtained directly are the RKM ternary *L*-parameters that are, as a function of temperature, as follows:

$$L^{(0)} = (14270 \pm 1270) + (100.1 \pm 7.6)T - (11.77 \pm 0.93)T\ln(T);$$

$$L^{(1)} = (145600 \pm 9780) + (101.6 \pm 58.7)T - (15.56 \pm 7.14)T\ln(T);$$

$$L^{(2)} = (76730 \pm 1240) + (79.2 \pm 7.4)T - (15.69 \pm 0.91)T\ln(T).$$

From the obtained ternary *L*-parameters the integral molar excess Gibbs energy, the excess chemical potentials, the activity coefficients and the activities have been evaluated. Using the temperature dependence of the activities, the integral and partial molar excess enthalpies and entropies can be also determined. In addition, for comparison, for some compositions, the Knudsen effusion isothermal evaporation method (IEM) and the Gibbs–Duhem ion intensity ratio method (GD-IIR) were used to determine activities and good agreement was obtained from the RKM model.

1. Introduction

The search for a replacement to lead solder in the electronic industry has increased significantly during the last decade. According to the European Waste from Electrical and Electronic Equipment ("WEEE") Directive (2002/96/EC) a ban was proposed on the use of Lead solders by January 2008. It is now widely agreed that there will be no single drop-in replacement for lead–tin solders and that the final choice of solder material will be application-dependent. Many people are beginning to investigate a number of possible replacements including binary, ternary and even quaternary alloy systems composed of Sn, Cu, Ag, In, Zn, Ni, Au and Pd. Indium is included here due to its low melting point while palladium, gold, copper and nickel also represent possible substrates. Albeit, neither the COST 531 nor the COST MP0602 actions selected Al as a possible candidate element the thermodynamic properties of Al–Cu–Sn system is still important in many industrial applications. In addition, we aim to demonstrate the capability of RKM-KEMS modelling on a system where all the pure components have approximately the same volatility so that all three components can be detected using the KEMS apparatus. The Al–Cu–Sn system satisfies this latter condition.

The full thermodynamic description of an alloy system is possible if one knows the Gibbs energy of all phases present in equilibrium at a given temperature. In this case, all binary combinations of possible elements have been studied using various methods to obtain their activities and other thermodynamic quantities of mixing. These data were then used to make a critical assessment of a particular binary system in the literature. As a result, a set of thermodynamic parameters is available to describe the phase equilibrium of binary systems. However, for ternary and quaternary systems, the greater number of solid phases makes the situation

* Corresponding author. Tel.: +36 1 3722500/1571; fax: +36 1 3722592.
E-mail address: bencze@chem.elte.hu (L. Bencze).

1387-3806/$ – see front matter © 2009 Elsevier B.V. All rights reserved.
doi:10.1016/j.ijms.2009.09.007

more complex and less experimental activity data and phase diagram information exist. In general, it is possible to obtain the interaction parameters from various experimental data including a phase diagram, chemical potential, thermodynamic activity, and enthalpy data by either trial and error or better still mathematically using the CALPHAD methods [1–3].

In 2001 Miki et al. [4] were able to show that by using the Redlich–Kister–Muggianu (RKM) sub-regular solution model they could obtain the ternary interaction parameters from direct mass spectrometric measurements. However, Miki et al. [4], as a simplification, assumed only one kind of ternary *L*-parameter instead of the generally accepted three different ones. In general, contrary to the assumptions by Miki et al. [4], the three ternary parameters are usually unequal. In addition, Miki et al. [4] determined a single ternary *L*-parameter and the corresponding thermodynamic data of mixing by measuring only the ion intensities of Ag^+ and In^+, *i.e.*, only the Ag^+ to In^+ ion intensity ratio. Recently, we applied Miki's [4] method to the study of the Cu–In–Sn system using only the Cu^+ to Sn^+ ion intensity ratio but we supplemented Miki's method assuming the classically three different ternary interaction parameters [5]. Later, in studying the Ag–In–Sn system [6] our aim was to elaborate on equivalent mathematical regression procedures using both the Ag^+ to Sn^+ and the Ag^+ to In^+ ion intensity ratios as independent input data, in order to study the mathematical relationship between the procedures based on both ion intensity ratios. In addition, we compared the data obtained by both procedures and in doing so confirmed the reliability of the data using the standard, model-free KEMS procedures. More recently, Schmidt and Tomiska [7] independently developed a similar mass spectrometric regression method not by using the RKM ternary *L*-parameters but by using the so called thermodynamic adoptive parameter series (TAP) for the description of the individual phases. Mixing thermodynamic data on the boundary binary systems (Al–Cu, Al–Sn and Cu–Sn) are available in several studies [8–11], whereas the data for Al–Cu–Sn is available only in Miettinen's work [12].

2. Experimental

A Nier type magnetic mass spectrometer was used in combination with a single Knudsen cell. The experimental technique is described in full elsewhere [13]. In a typical experiment, the sample is heated in the Knudsen cell to the desired temperature. Vapour species, effusing through a small cell orifice (¢: 0.5 mm), are admitted into the ionisation chamber of the ion source where they are ionised (30 eV) and form an ion beam in the ion optics of the ion source. The ion beam is then separated in the analyser according to the mass-to-charge ratios of the ions and the ion intensities are measured using an electron multiplier. The multiplier (ETP type) was operated in the counting mode at −3.0 kV feed. For a detailed description of the experimental set-up see Ref. [14]. In such an arrangement, above the condensed sample, the equilibrium vapour pressure (p_j) of the molecular species '*j*', within the Knudsen cell, can be obtained using the following equation

$$p_j = \frac{KT}{\sigma_j} \sum_k \frac{I_{jk}^+}{\eta_k \gamma_k} \tag{1}$$

where I_{jk}^+ is the intensity of ion *k* formed from the molecular species *j*; *T* is the absolute temperature of the Knudsen cell; *K* the general sensitivity constant of the instrument; σ_j the ionisation cross-section of molecular species *j* at the measured ionising electron energy; η_k and γ_k the isotope abundance and the multiplier efficiency for ion *k*; respectively. At the counting mode and optimal supply voltage γ_k was the same for all kinds of ions.

We can also obtain the variation of the vapour pressure ratio of two given species with temperature by measuring the ion intensity ratio belonging to these species without explicit knowledge of the values of the parameters in Eq. (1). This important feature of KEMS, as a relative method, makes it an efficient technique for measuring the activities and thermodynamic quantities of binary systems [15]. Using the relative KEMS methods it is not necessary to calculate the vapour pressures of the components, since the activities can be obtained directly from the measured ion intensities or ion intensity ratios.

3. Sample preparation and measuring procedure

Weighted amounts of powdered pure metals obtained from SIGMA-ALDRICH (500 mg of total mass) were mixed and made into pellets at room temperature. During the application of high pressure the small grains became sintered. Each pellet was then loaded into a cylindrical alumina cell (10 mm long, 10 mm in diameter) having a channel-type orifice diameter of 0.5 mm and length of 1.4 mm. The cell was then inserted into the Knudsen evaporator [14], evacuated to high vacuum and heated to 1200 °C at 20 °C/min. Due to the sintering of the grains under pressure the mixtures became completely homogeneous liquid at around their liquidus temperatures, *i.e.*, below 1000 °C at all compositions. Soon after reaching 1200 °C and thermodynamic equilibrium the intensities of $^{27}Al^+$, $^{63}Cu^+$ and $^{120}Sn^+$ ions were measured at every 10 °C down to 1000 °C. 1200 °C is much higher temperature than the liquidus temperature at any composition. For the isothermal evaporation experiments two kinds of alumina cells, differing in construction and geometry, were used.

4. Determination of thermodynamic quantities of mixing by conventional KEMS methods and a new method based on applying the Redlich–Kister–Muggianu sub-regular solution model

The excess Gibbs energy of ternary liquid mixtures, taking both binary and ternary interactions into account, can be described as random mixtures of components *A*, *B* and *C* by a sub-regular-solution type model after Muggianu [16] as

$$G^{\mathrm{E}} = X_{\mathrm{A}}X_{\mathrm{B}} \sum_{i=0}^{n_{\mathrm{AB}}} L_{\mathrm{AB}}^{(i)} (X_{\mathrm{A}} - X_{\mathrm{B}})^i + X_{\mathrm{A}}X_{\mathrm{C}} \sum_{i=0}^{n_{\mathrm{AC}}} L_{\mathrm{AC}}^{(i)} (X_{\mathrm{A}} - X_{\mathrm{C}})^i + X_{\mathrm{B}}X_{\mathrm{C}} \sum_{i=0}^{n_{\mathrm{BC}}} L_{\mathrm{BC}}^{(i)} (X_{\mathrm{B}} - X_{\mathrm{C}})^i + X_{\mathrm{A}}X_{\mathrm{B}}X_{\mathrm{C}} [L_{\mathrm{ABC}}^{(0)} X_{\mathrm{A}} + L_{\mathrm{ABC}}^{(1)} X_{\mathrm{B}} + L_{\mathrm{ABC}}^{(2)} X_{\mathrm{C}}] \tag{2}$$

where X_{A}, X_{B} and X_{C} are the mole fractions, and the *Ls* are the binary and ternary interaction parameters. In a real system the notations A, B and C must be replaced with the formulae of the real components (in our case elements) in alphabetic order, *e.g.*, A = Al, B = Cu and C = Sn. While the number of the binary *L*-parameters (n_{AB}, n_{AC} and n_{BC}) used in Eq. (2) depends on the best fit for the measured G^{E} binary data, the number of the ternary *L*-parameters is strictly three. For an explanation, see the Appendix. Nevertheless, in simplified cases only one ternary L_{ABC} is assumed (Miki et al.'s [4] assumption: $L_{\mathrm{ABC}}^{(0)} = L_{\mathrm{ABC}}^{(1)} = L_{\mathrm{ABC}}^{(2)} = L_{\mathrm{ABC}}$, *see e.g.*, Ref. [4]).

In our previous work [6] we have derived expressions of how to use different ion intensity ratios (*e.g.*, Ag^+ to In^+ or Ag^+ to Sn^+) independently for the least-squares determination of the theoretically same ternary *Ls* and the thermodynamic properties. Applying these expressions to the Al–Cu–Sn system the following equations are obtained using the Al^+ to Sn^+ ion intensity ratio, called as '*Al^+/Sn^+ method*':

$$Ysumma_{\mathrm{AlCuSn}(Al^+/Sn^+)}$$

$$= -C_{\mathrm{AlCuSn(Al^+/Sn^+)}} + L^{(0)}_{\mathrm{AlCuSn}}(2X_{\mathrm{Sn}} - X_{\mathrm{Al}})X_{\mathrm{Al}}X_{\mathrm{Cu}}$$
$$+ L^{(1)}_{\mathrm{AlCuSn}}(X_{\mathrm{Sn}} - X_{\mathrm{Al}})(X_{\mathrm{Cu}})^2 + L^{(2)}_{\mathrm{AlCuSn}}(X_{\mathrm{Sn}} - 2X_{\mathrm{Al}})X_{\mathrm{Sn}}X_{\mathrm{Cu}} \quad (3)$$

where $Ysumma_{\mathrm{AlCuSn(Al^+/Sn^+)}}$, $YY_{\mathrm{AlCuSn(Al^+/Sn^+)}}$ and $Y_{\mathrm{AlCuSn(Al^+/Sn^+)}}$ can be determined using Eqs. (4)–(6) below:

$$Ysumma_{\mathrm{AgInSn(Al^+/Sn^+)}} \equiv Y_{\mathrm{AgInSn(Al^+/Sn^+)}} + YY_{\mathrm{AgInSn(Al^+/Sn^+)}} \quad (4)$$

$$YY_{\mathrm{AgInSn(Al^+/Sn^+)}} \equiv RT \ln\left(\frac{I_{\mathrm{Al}}X_{\mathrm{Sn}}}{I_{\mathrm{Sn}}X_{\mathrm{Al}}}\right) \quad (5)$$

$$\begin{aligned} Y_{\mathrm{AlCuSn(Al^+/Sn^+)}} \equiv & -\{X_{\mathrm{Cu}}[L^{(0)}_{\mathrm{AlCu}} + L^{(1)}_{\mathrm{AlCu}}(X_{\mathrm{Al}} - X_{\mathrm{Cu}}) \\ & + L^{(2)}_{\mathrm{AlCu}}(X_{\mathrm{Al}} - X_{\mathrm{Cu}})^2 + L^{(3)}_{\mathrm{AlCu}}(X_{\mathrm{Al}} - X_{\mathrm{Cu}})^3] \\ & + X_{\mathrm{Al}}X_{\mathrm{Cu}}[L^{(1)}_{\mathrm{AlCu}} + 2L^{(2)}_{\mathrm{AlCu}}(X_{\mathrm{Al}} - X_{\mathrm{Cu}}) \\ & + 3L^{(3)}_{\mathrm{AlCu}}(X_{\mathrm{Al}} - X_{\mathrm{Cu}})^2] + (1 - X_{\mathrm{Cu}} - 2X_{\mathrm{Al}}) \\ & \times [L^{(0)}_{\mathrm{AlSn}} + L^{(1)}_{\mathrm{AlSn}}(2X_{\mathrm{Al}} - 1 + X_{\mathrm{Cu}}) \\ & + L^{(2)}_{\mathrm{AlSn}}(2X_{\mathrm{Al}} - 1 + X_{\mathrm{Cu}})^2 + L^{(3)}_{\mathrm{AlSn}}(2X_{\mathrm{Al}} - 1 + X_{\mathrm{Cu}})^3] \\ & + X_{\mathrm{Al}}(1 - X_{\mathrm{Cu}} - X_{\mathrm{Al}})[2L^{(1)}_{\mathrm{AlSn}} \\ & + 4L^{(2)}_{\mathrm{AlSn}}(2X_{\mathrm{Al}} - 1 + X_{\mathrm{Cu}}) \\ & + 6L^{(3)}_{\mathrm{AlSn}}(2X_{\mathrm{Al}} - 1 + X_{\mathrm{Cu}})^2] \\ & - X_{\mathrm{Cu}}[L^{(0)}_{\mathrm{CuSn}} + L^{(1)}_{\mathrm{CuSn}}(3X_{\mathrm{Cu}} - 2 + 2X_{\mathrm{Al}})]\} \end{aligned} \quad (6a)$$

when $L^{(3)}_{\mathrm{CuSn}}$ and $L^{(2)}_{\mathrm{CuSn}}$ are considered as zero. Nevertheless, if some more binary *Ls* are zero (like $L^{(3)}_{\mathrm{AlCu}}$ and $L^{(3)}_{\mathrm{AlSn}}$ in the COST 507 [8] database and in Miettinen' s paper [12], as well as $L^{(3)}_{\mathrm{CuSn}}$ in the COST 531 [9] database (see Table 2)) the expressions including the quantities in Eq. (6a) are also zero. In contrast, the binary $L^{(3)}_{\mathrm{CuSn}}$ and $L^{(2)}_{\mathrm{CuSn}}$ data, obtained by Witusiewicz et al. [10], Miettinen [12], and in this work using a multiple regression on Hultgren' s original data [11], are not zero (see Table 2). Therefore, an equation assuming a non-zero $L^{(3)}$ data must be derived. Nevertheless, it is usually not necessary to describe G^{E} of the binary systems using power 4 in the polynomials.

By assuming that none of the $L^{(3)}$ data have non-zero values, by applying the relation between the three mole fractions and distributing the 5-term-equation, *i.e.*, Eq. (6a) to a 7-term-one for easier comparison, the latter equation changes to Eq. (6b) as follows:

$$\begin{aligned} Y_{\mathrm{AlCuSn(Al^+/Sn^+)}} \equiv & -\{X_{\mathrm{Cu}}[L^{(0)}_{\mathrm{AlCu}} + L^{(1)}_{\mathrm{AlCu}}(X_{\mathrm{Al}} - X_{\mathrm{Cu}}) + L^{(2)}_{\mathrm{AlCu}}(X_{\mathrm{Al}} - X_{\mathrm{Cu}})^2 \\ & + L^{(3)}_{\mathrm{AlCu}}(X_{\mathrm{Al}} - X_{\mathrm{Cu}})^3] + X_{\mathrm{Al}}X_{\mathrm{Cu}}[L^{(1)}_{\mathrm{AlCu}} \\ & + 2L^{(2)}_{\mathrm{AlCu}}(X_{\mathrm{Al}} - X_{\mathrm{Cu}}) + 3L^{(3)}_{\mathrm{AlCu}}(X_{\mathrm{Al}} - X_{\mathrm{Cu}})^2] \\ & + X_{\mathrm{Sn}}[L^{(0)}_{\mathrm{AlSn}} + L^{(1)}_{\mathrm{AlSn}}(X_{\mathrm{Al}} - X_{\mathrm{Sn}}) \\ & + L^{(2)}_{\mathrm{AlSn}}(X_{\mathrm{Al}} - X_{\mathrm{Sn}})^2 + L^{(3)}_{\mathrm{AlSn}}(X_{\mathrm{Al}} - X_{\mathrm{Sn}})^3] \\ & - X_{\mathrm{Al}}[L^{(0)}_{\mathrm{AlSn}} + L^{(1)}_{\mathrm{AlSn}}(X_{\mathrm{Al}} - X_{\mathrm{Sn}}) \\ & + L^{(2)}_{\mathrm{AlSn}}(X_{\mathrm{Al}} - X_{\mathrm{Sn}})^2 + L^{(3)}_{\mathrm{AlSn}}(X_{\mathrm{Al}} - X_{\mathrm{Sn}})^3] \\ & + X_{\mathrm{Al}}X_{\mathrm{Sn}}[2L^{(1)}_{\mathrm{AlSn}} + 4L^{(2)}_{\mathrm{AlSn}}(X_{\mathrm{Al}} - X_{\mathrm{Sn}}) \\ & + 6L^{(3)}_{\mathrm{AlSn}}(X_{\mathrm{Al}} - X_{\mathrm{Sn}})^2] - X_{\mathrm{Cu}}[L^{(0)}_{\mathrm{CuSn}} \\ & + L^{(1)}_{\mathrm{CuSn}}(X_{\mathrm{Cu}} - X_{\mathrm{Sn}}) \\ & + L^{(2)}_{\mathrm{CuSn}}(X_{\mathrm{Cu}} - X_{\mathrm{Sn}})^2 + L^{(3)}_{\mathrm{CuSn}}(X_{\mathrm{Cu}} - X_{\mathrm{Sn}})^3] \\ & + X_{\mathrm{Cu}}X_{\mathrm{Sn}}[L^{(1)}_{\mathrm{CuSn}} + 2L^{(2)}_{\mathrm{CuSn}}(X_{\mathrm{Cu}} - X_{\mathrm{Sn}}) \\ & + 3L^{(3)}_{\mathrm{CuSn}}(X_{\mathrm{Cu}} - X_{\mathrm{Sn}})^2]\} \end{aligned} \quad (6b)$$

When Al^+ and Cu^+ are measured, the three ternary *L*-parameters should be determined using Eq. (7), also called as the '*Al^+/Cu^+ method*':

$$\begin{aligned} & Ysumma_{\mathrm{AlCuSn(Al^+/Cu^+)}} \\ & = -C_{\mathrm{AlCuSn(Al^+/Cu^+)}} + L^{(0)}_{\mathrm{AlCuSn}}(2X_{\mathrm{Cu}} - X_{\mathrm{Al}})X_{\mathrm{Al}}X_{\mathrm{Cu}} \\ & \quad + L^{(1)}_{\mathrm{AlCuSn}}(X_{\mathrm{Cu}} - 2X_{\mathrm{Al}})X_{\mathrm{Sn}}X_{\mathrm{Cu}} + L^{(2)}_{\mathrm{AlCuSn}}(X_{\mathrm{Cu}} - X_{\mathrm{Al}})(X_{\mathrm{Sn}})^2 \end{aligned} \quad (7)$$

where $Ysumma_{\mathrm{AlCuSn(Al^+/Cu^+)}}$, $YY_{\mathrm{AlCuSn(Al^+/Cu^+)}}$ and $Y_{\mathrm{AlCuSn(Al^+/Cu^+)}}$ can be determined using Eqs. (8)–(10) below:

$$Ysumma_{\mathrm{AlCuSn(Al^+/Cu^+)}} \equiv Y_{\mathrm{AlCuSn(Al^+/Cu^+)}} + YY_{\mathrm{AlCuSn(Al^+/Cu^+)}} \quad (8)$$

$$YY_{\mathrm{AlCuSn(Al^+/Cu^+)}} \equiv RT \ln\left(\frac{I_{\mathrm{Al}}X_{\mathrm{Cu}}}{I_{\mathrm{Cu}}X_{\mathrm{Al}}}\right) \quad (9)$$

$$\begin{aligned} & Y_{\mathrm{AlCuSn(Al^+/Cu^+)}} \\ & \equiv -\{X_{\mathrm{Cu}}[L^{(0)}_{\mathrm{AlCu}} + L^{(1)}_{\mathrm{AlCu}}(X_{\mathrm{Al}} - X_{\mathrm{Cu}}) + L^{(2)}_{\mathrm{AlCu}}(X_{\mathrm{Al}} - X_{\mathrm{Cu}})^2 \\ & \quad + L^{(3)}_{\mathrm{AlCu}}(X_{\mathrm{Al}} - X_{\mathrm{Cu}})^3] + X_{\mathrm{Al}}X_{\mathrm{Sn}}[L^{(1)}_{\mathrm{AlSn}} + 2L^{(2)}_{\mathrm{AlSn}}(X_{\mathrm{Al}} - X_{\mathrm{Sn}}) \\ & \quad + 3L^{(3)}_{\mathrm{AlSn}}(X_{\mathrm{Al}} - X_{\mathrm{Sn}})^2] + X_{\mathrm{Sn}}[L^{(0)}_{\mathrm{AlSn}} + L^{(1)}_{\mathrm{AlSn}}(X_{\mathrm{Al}} - X_{\mathrm{Sn}}) \\ & \quad + L^{(2)}_{\mathrm{AlSn}}(X_{\mathrm{Al}} - X_{\mathrm{Sn}})^2 + L^{(3)}_{\mathrm{AlSn}}(X_{\mathrm{Al}} - X_{\mathrm{Sn}})^3] - X_{\mathrm{Al}}[L^{(0)}_{\mathrm{AlCu}} \\ & \quad + L^{(1)}_{\mathrm{AlCu}}(X_{\mathrm{Al}} - X_{\mathrm{Cu}}) + L^{(2)}_{\mathrm{AlCu}}(X_{\mathrm{Al}} - X_{\mathrm{Cu}})^2 + L^{(3)}_{\mathrm{AlCu}}(X_{\mathrm{Al}} - X_{\mathrm{Cu}})^3] \\ & \quad + X_{\mathrm{Al}}X_{\mathrm{Cu}}[2L^{(1)}_{\mathrm{AlCu}} + 4L^{(2)}_{\mathrm{AlCu}}(X_{\mathrm{Al}} - X_{\mathrm{Cu}}) + 6L^{(3)}_{\mathrm{AlCu}}(X_{\mathrm{Al}} - X_{\mathrm{Cu}})^2] \\ & \quad - X_{\mathrm{Sn}}[L^{(0)}_{\mathrm{CuSn}} + L^{(1)}_{\mathrm{CuSn}}(X_{\mathrm{Cu}} - X_{\mathrm{Sn}}) + L^{(2)}_{\mathrm{CuSn}}(X_{\mathrm{Cu}} - X_{\mathrm{Sn}})^2 \\ & \quad + L^{(3)}_{\mathrm{CuSn}}(X_{\mathrm{Cu}} - X_{\mathrm{Sn}})^3] - X_{\mathrm{Cu}}X_{\mathrm{Sn}}[L^{(1)}_{\mathrm{CuSn}} + 2L^{(2)}_{\mathrm{CuSn}}(X_{\mathrm{Cu}} - X_{\mathrm{Sn}}) \\ & \quad + 3L^{(3)}_{\mathrm{CuSn}}(X_{\mathrm{Cu}} - X_{\mathrm{Sn}})^2]\} \end{aligned} \quad (10)$$

Comparing Eq. (10) to Eq. (6b) certain construction relationships become apparent. Eq. (10) can be obtained from Eq. (6b) by replacing Cu with Sn and Sn with Cu. A relationship also exists between Eqs. (3) and (7): in addition to the exchange of subscripts Sn and Cu in the mole fractions, the multipliers of $L^{(1)}_{\mathrm{AlCuSn}}$ and $L^{(2)}_{\mathrm{AlCuSn}}$ are also exchanged.

Notable is that the $L^{(0)}_{\mathrm{AlCuSn}}$, $L^{(1)}_{\mathrm{AlCuSn}}$ and $L^{(2)}_{\mathrm{AlCuSn}}$ ternary parameters can be obtained from both Eqs. (3) and (7) by multiple regression on different functions. This is the advantage of KEMS, *i.e.*, it is possible to use the complete mass spectrum for the parallel determination of the ternary *Ls*. The regression matrix equation based on Eqs. (3) and (7), can be expressed by Eqs. (11) and (12) as follows:

$$\begin{bmatrix} 1 & ((2X_{\mathrm{Sn}} - X_{\mathrm{Al}})X_{\mathrm{Al}}X_{\mathrm{Cu}})_1 & ((X_{\mathrm{Sn}} - X_{\mathrm{Al}})X^2_{\mathrm{Cu}})_1 & ((X_{\mathrm{Sn}} - 2X_{\mathrm{Al}})X_{\mathrm{Sn}}X_{\mathrm{Cu}})_1 \\ 1 & ((2X_{\mathrm{Sn}} - X_{\mathrm{Al}})X_{\mathrm{Al}}X_{\mathrm{Cu}})_2 & ((X_{\mathrm{Sn}} - X_{\mathrm{Al}})X^2_{\mathrm{Cu}})_2 & ((X_{\mathrm{Sn}} - 2X_{\mathrm{Al}})X_{\mathrm{Sn}}X_{\mathrm{Cu}})_2 \\ \vdots & \vdots & \vdots & \vdots \\ 1 & ((2X_{\mathrm{Sn}} - X_{\mathrm{Al}})X_{\mathrm{Al}}X_{\mathrm{Cu}})_n & ((X_{\mathrm{Sn}} - X_{\mathrm{Al}})X^2_{\mathrm{Cu}})_n & ((X_{\mathrm{Sn}} - 2X_{\mathrm{Al}})X_{\mathrm{Sn}}X_{\mathrm{Cu}})_n \end{bmatrix} \begin{bmatrix} -C \\ L^{(0)}_{\mathrm{AlCuSn}} \\ L^{(1)}_{\mathrm{AlCuSn}} \\ L^{(2)}_{\mathrm{AlCuSn}} \end{bmatrix}$$
$$= \begin{bmatrix} Ysumma_{(\mathrm{Al^+/Sn^+})_1} \\ Ysumma_{(\mathrm{Al^+/Sn^+})_2} \\ \vdots \\ Ysumma_{(\mathrm{Al^+/Sn^+})_n} \end{bmatrix} \quad (11)$$

$$\begin{bmatrix} 1 & ((2X_{Cu}-X_{Al})X_{Al}X_{Sn})_1 & ((X_{Cu}-2X_{Al})X_{Cu}X_{Sn})_1 & ((X_{Cu}-X_{Al})X_{Sn}^2)_1 \\ 1 & ((2X_{Cu}-X_{Al})X_{Al}X_{Sn})_2 & ((X_{Cu}-2X_{Al})X_{Cu}X_{Sn})_2 & ((X_{Cu}-X_{Al})X_{Sn}^2)_2 \\ \vdots & \vdots & \vdots & \vdots \\ 1 & ((2X_{Cu}-X_{Al})X_{Al}X_{Sn})_n & ((X_{Cu}-2X_{Al})X_{Cu}X_{Sn})_n & ((X_{Cu}-X_{Al})X_{Sn}^2)_n \end{bmatrix} \begin{bmatrix} -C \\ L^{(0)}_{AlCuSn} \\ L^{(1)}_{AlCuSn} \\ L^{(2)}_{AlCuSn} \end{bmatrix} = \begin{bmatrix} Ysumma_{(Al^+/Cu^+)_1} \\ Ysumma_{(Al^+/Cu^+)_2} \\ \vdots \\ Ysumma_{(Al^+/Cu^+)_n} \end{bmatrix} \quad (12)$$

In order to decrease the uncertainties of $L^{(0)}_{AlCuSn}$, $L^{(1)}_{AlCuSn}$ and $L^{(2)}_{AlCuSn}$ determined by the separate Al^+/Sn^+ and Al^+/Cu^+ methods, Eqs. (3) and (7) can either be added or extracted. Using the addition method, double the amount of measured input data can be used for a joint multiple regression. The equations of this '*addition method*' are as follows:

$$\begin{aligned} Ysumma_{added} &= -C_{added} + L^{(0)}_{AlCuSn}(4X_{Al}X_{Cu}X_{Sn} - X_{Al}^2(1-X_{Al})) \\ &\quad + L^{(1)}_{AlCuSn}(2X_{Cu}X_{Sn} - X_{Al}X_{Cu} - 2X_{Al}X_{Sn})X_{Cu} \\ &\quad + L^{(2)}_{AlCuSn}(2X_{Cu}X_{Sn} - X_{Al}X_{Sn} - 2X_{Al}X_{Cu})X_{Sn} \end{aligned} \quad (13)$$

where

$$\begin{aligned} Ysumma_{added} &= Ysumma_{AlCuSn(Al^+/Sn^+)} + Ysumma_{AlCuSn(Al^+//Cu^+)} \\ &= Y_{AlCuSn(Al^+/Sn^+)} + YY_{AlCuSn(Al^+/Sn^+)} + Y_{AlCuSn(Al^+/Cu^+)} \\ &\quad + YY_{AlCuSn(Al^+/Cu^+)} \equiv Y_{added} + YY_{added} \end{aligned} \quad (14)$$

$$C_{added} = C_{AlCuSn(Al^+/Sn^+)} + C_{AlCuSn(Al^+//Cu^+)} \quad (15)$$

The only disadvantage of this 'addition method' is that C_{added}, obtained by multiple regression using Eq. (13), cannot be apportioned to $C_{AlCuSn(Al^+/Sn^+)}$ and $C_{AlCuSn(Al^+/Cu^+)}$. This means that the latter two quantities, and hence, also the σ_{Al}/σ_{Sn} and σ_{Al}/σ_{Cu} mass spectrometric ionisation cross-section ratios, that are in mathematical relation with $C_{AlCuSn(Al^+/Sn^+)}$ and $C_{AlCuSn(Al^+/Cu^+)}$, cannot be separately determined.

Instead of adding Eqs. (3) and (7) it is possible also to extract them but in this case actually the measured aluminium ion intensity data are not used for the further calculations since they are omitted as follows:

$$\begin{aligned} YY_{extracted} &= YY_{AlCuSn(Al^+/Sn^+)} - YY_{AlCuSn(Al^+/Cu^+)} \\ &= RT\ln\left(\frac{I_{Al}X_{Sn}}{I_{Sn}X_{Al}}\right) - RT\ln\left(\frac{I_{Al}X_{Cu}}{I_{Cu}X_{Al}}\right) \\ &= RT\ln\left(\frac{I_{Cu}X_{Sn}}{I_{Sn}X_{Cu}}\right) \equiv YY_{AlCuSn(Cu^+/Sn^+)} \end{aligned} \quad (16)$$

The extraction method actually leads to the so called '*Cu^+/Sn^+ method*' since it leads to the elimination of the Al^+ ion intensity data. Using this method means there is no doubling in the amount of input data (*i.e.*, two kinds of ion intensity ratios) for the multiple regression but only a single set of input data, the Cu^+/Sn^+ ion intensity ratio data. Obviously, in a ternary system there are only two independent ion intensity ratios, *i.e.*, the third intensity ratio variant depends on the other two. The regression equation for this '*Cu^+/Sn^+ method*' can be derived as follows:

$$\begin{aligned} Ysumma_{extracted} &= -C_{extracted} + L^{(0)}_{AlCuSn}X_{Al}^2(X_{Sn}-X_{Cu}) \\ &\quad + L^{(1)}_{AlCuSn}X_{Al}X_{Cu}(2X_{Sn}-X_{Cu}) \\ &\quad + L^{(2)}_{AlCuSn}X_{Al}X_{Sn}(X_{Sn}-2X_{Cu}) \end{aligned} \quad (17)$$

where

$$\begin{aligned} Ysumma_{extracted} &= Ysumma_{AlCuSn(Al^+/Sn^+)} - Ysumma_{AlCuSn(Al^+/Cu^+)} \\ &\equiv Ysumma_{AlCuSn(Cu^+/Sn^+)} = (Y_{AlCuSn(Al^+/Sn^+)} \\ &\quad + YY_{AlCuSn(Al^+/Sn^+)}) - (Y_{AlCuSn(Al^+/Cu^+)} \\ &\quad + YY_{AlCuSn(Al^+/Cu^+)}) = Y_{extracted} + YY_{extracted} \\ &\equiv Y_{AlCuSn(Cu^+/Sn^+)} + YY_{AlCuSn(Cu^+/Sn^+)} \end{aligned} \quad (18)$$

$$C_{extracted} = C_{AlCuSn(Al^+/Sn^+)} - C_{AlCuSn(Al^+/Cu^+)} \equiv C_{AlCuSn(Cu^+/Sn^+)} \quad (19)$$

$$\begin{aligned} &Y_{AlCuSn(Cu^+/Sn^+)} \\ &\equiv -X_{Al}X_{Sn}[L^{(1)}_{AlSn} + 2L^{(2)}_{AlSn}(X_{Al}-X_{Sn}) + 3L^{(3)}_{AlSn}(X_{Al}-X_{Sn})^2] \\ &\quad - X_{Al}[L^{(0)}_{AlCu} + L^{(1)}_{AlCu}(X_{Al}-X_{Cu}) + L^{(2)}_{AlCu}(X_{Al}-X_{Cu})^2 \\ &\quad + L^{(3)}_{AlCu}(X_{Al}-X_{Cu})^3] + X_{Al}[L^{(0)}_{AlSn} + L^{(1)}_{AlSn}(X_{Al}-X_{Sn}) \\ &\quad + L^{(2)}_{AlSn}(X_{Al}-X_{Sn})^2 + L^{(3)}_{AlSn}(X_{Al}-X_{Sn})^3] \\ &\quad + X_{Cu}[L^{(0)}_{CuSn} + L^{(1)}_{CuSn}(X_{Cu}-X_{Sn}) + L^{(2)}_{CuSn}(X_{Cu}-X_{Sn})^2 \\ &\quad + L^{(3)}_{CuSn}(X_{Cu}-X_{Sn})^3] + X_{Al}X_{Cu}[L^{(1)}_{AlCu} + 2L^{(2)}_{AlCu}(X_{Al}-X_{Cu}) \\ &\quad + 3L^{(3)}_{AlCu}(X_{Al}-X_{Cu})^2] - X_{Sn}[L^{(0)}_{CuSn} + L^{(1)}_{CuSn}(X_{Cu}-X_{Sn}) \\ &\quad + L^{(2)}_{CuSn}(X_{Cu}-X_{Sn})^2 + L^{(3)}_{CuSn}(X_{Cu}-X_{Sn})^3] \\ &\quad - X_{Cu}X_{Sn}[2L^{(1)}_{CuSn} + 4L^{(2)}_{CuSn}(X_{Cu}-X_{Sn}) + 6L^{(3)}_{CuSn}(X_{Cu}-X_{Sn})^2] \end{aligned} \quad (20)$$

By using the ternary *L*s obtained by any of the Eqs. (3), (7), (13) or (17) it is possible to obtain the excess Gibbs energy using Eq. (2). From this it is possible to determine the excess chemical potentials, the activity coefficients and the activities using the following well-known thermodynamic relationships (21)–(24):

$$a_i = X_i\gamma_i = X_i\exp\left(\frac{\mu_i^E}{RT}\right) \quad (21)$$

$$\mu_{Al}^E = G^E - X_{Cu}\left(\frac{\partial G^E}{\partial X_{Cu}}\right)_{X_{Al}} + (1-X_{Al})\left(\frac{\partial G^E}{\partial X_{Al}}\right)_{X_{Cu}} \quad (22)$$

$$\mu_{Sn}^E = G^E - X_{Al}\left(\frac{\partial G^E}{\partial X_{Al}}\right)_{X_{Cu}} - X_{Cu}\left(\frac{\partial G^E}{\partial X_{Cu}}\right)_{X_{Al}} \quad (23)$$

$$\mu_{Cu}^E = G^E - X_{Al}\left(\frac{\partial G^E}{\partial X_{Al}}\right)_{X_{Sn}} - X_{Sn}\left(\frac{\partial G^E}{\partial X_{Sn}}\right)_{X_{Al}} \quad (24)$$

where *i* denotes any of the components (Al, Cu or Sn). In addition, it is also possible to obtain the partial molar and integral molar excess enthalpies and entropies from the temperature dependence of these quantities using the well-known Gibbs–Helmholtz equation.

Other KEMS experiments, involving determining activities, were performed using the conventional Knudsen effusion isothermal evaporation method (IEM) [13]. This method involves measuring the rate of total mass loss of the alloy and measuring the mass spectrum of the equilibrium vapour (IEM-KEMS). An alternative possibility for determining the equilibrium partial pressures is, instead of obtaining the mass spectrum, to analyse the vapour deposit (IEM-VDA). Popovic [14] was the first to develop this technique using a Knudsen effusion mass spectrometer for the determination of equilibrium partial pressures over a condensed

mixture. This technique means it now possible to determine the relative ionisation cross-sections of the gas phase molecules present in a gas mixture. The method needs a Knudsen evaporator in a high vacuum system but it does not require a mass spectrometer. Nevertheless, the IEM-VDA experiments were made in the same KEMS apparatus. The realisation of this method in our KEMS apparatus was such that sticky-tape was fixed onto the water-cooled inner wall of the mass spectrometer, with the tape facing the molecular beam of the vapour mixture. Vapours from the alloy, crossing the ionisation chamber, condensed on the cold tape, forming a thin, mixed metal film. This film was then dissolved off the tape using appropriate acids and the metal composition of the solution analysed using inductively coupled plasma atomic emission spectroscopy (ICP-AOS). An alternative method analysing the mixed metal film is neutron activation analysis (NAA), which has the advantage of not corroding the film. Therefore, we applied first NAA and then, as a confirmatory method, ICP-AOS. By applying both methods, the uncertainties in the concentration data can be reduced.

Mass loss is due to the long-term isothermal evaporation from the Knudsen cell—the vapours leave the cell through the orifice. If the mass spectrum (the ion intensities of all the components) is also measured simultaneously (IEM-KEMS) the partial pressures, and therefore, the thermodynamic activities can be determined using the well-known Hertz–Knudsen equation assuming no compositional shift, as follows:

$$p_{Al} = \frac{KT}{\sigma_{Al}\eta_{Al^+}\gamma_{Al^+}} I_{Al^+}, \quad p_{Cu} = \frac{KT}{\sigma_{Cu}\eta_{Cu^+}\gamma_{Cu^+}} I_{Cu^+},$$

$$p_{Sn} = \frac{KT}{\sigma_{Sn}\eta_{Sn^+}\gamma_{Sn^+}} I_{Sn^+} \quad \text{where}$$

$$K = \sqrt{\frac{2\pi R}{T}} \frac{\Delta m}{CA\,\Delta t} \left(\frac{I_{Al^+}}{\sigma_{Al}\eta_{Al^+}\gamma_{Al^+}} \sqrt{M_{Al}} + \frac{I_{Cu^+}}{\sigma_{Cu}\eta_{Cu^+}\gamma_{Cu^+}} \sqrt{M_{Cu}} + \frac{I_{Sn^+}}{\sigma_{Sn}\eta_{Sn^+}\gamma_{Sn^+}} \sqrt{M_{Sn}} \right)^{-1} \tag{25}$$

where Δm is the total mass loss, Δt is the duration of the isothermal evaporation experiment, K is the sensitivity constant of the mass spectrometer, M is the molar mass of an effusing gaseous species, A is the area of the orifice of the Knudsen cell, C is the Clausing factor of the orifice, R is the universal gas constant. The term M denotes the mean molar mass if the effusing species are not mono-isotopic whereas the ion intensity (I) and the detector (multiplier) gain factor (γ) belong to the measured (selected) isotopic ion. A correction of the selected isotopic ion intensity to the total ion intensity is performed using the isotopic abundance factor (η).

Since the differences in volatility among the components of Al–Cu–Sn is low, the total mass loss, that can simply be measured using an analytical balance before and after the isothermal evaporation experiment, consists of comparable partial mass losses of the components. If we combine the measurement of the total mass loss with the chemical analysis of the vapour deposit rather than with the mass spectrum, the equations for determining partial pressures are as follows:

$$\Delta m = \Delta m_{Al} + \Delta m_{Cu} + \Delta m_{Sn} \tag{26}$$

$$p_{Al} = \frac{\Delta m_{Al}}{CA\,\Delta t}\sqrt{\frac{2\pi RT}{M_{Al}}}, \quad p_{Cu} = \frac{\Delta m_{Cu}}{CA\,\Delta t}\sqrt{\frac{2\pi RT}{M_{Cu}}},$$

$$p_{Sn} = \frac{\Delta m_{Sn}}{CA\,\Delta t}\sqrt{\frac{2\pi RT}{M_{Sn}}} \tag{27}$$

$$a_{Al} = \frac{p_{Al}}{p^*_{Al}} \quad \text{and} \quad a_{Cu} = \frac{p_{Cu}}{p^*_{Cu}} \quad \text{and} \quad a_{Sn} = \frac{p_{Sn}}{p^*_{Sn}} \tag{28}$$

where Δm_{Al}, Δm_{Cu} and Δm_{Sn} are the partial mass losses of Al, Cu and Sn, respectively, and are obtained from the total mass loss and the elementary analysis of the vapour deposit. p^*_{Al}, p^*_{Cu} and p^*_{Sn}, which are the vapour pressures of pure Al, Cu and Sn, respectively, can be obtained either from the literature or by performing our own measurements as follows:

If evaporation experiments with pure components are also made at the same temperature and using the same Knudsen cell like that used for the alloy samples, it is not necessary to determine the Clausing factor of the orifice (C) and the orifice area (A) since they are omitted by applying Eq. (27) for both pure metal and the alloy:

$$a_{Me} = \frac{p_{Me}}{p^*_{Me}} = \frac{dm_{Me}/dt}{(dm_{Me}/dt)^*} \approx \frac{\Delta m_{Me}/\Delta t}{(\Delta m_{Me}/\Delta t)^*} \tag{29}$$

where Me denotes either Al, Cu or Sn and the asterisk (*) denotes the pure component.

Using the IEM-VDA method it is possible to avoid the use of literature ionisation cross-sections in order to decrease the systematic error in the thermodynamic data. We performed isothermal evaporation experiments at 1453 K (1180 °C). The above-mentioned equations are valid only if no significant compositional shift (distillation) occurs during the IEM experiments. A typical mass loss from a starting 1000 mg of sample was 10 mg. Therefore, we required practically no compositional correction. Also, if the volatility of a component is much higher (*i.e.*, orders of magnitude,) than that of the other ones this method does not require the measurement of the mass spectrum or the analysis of the vapour deposit (*see* Refs. [5,6]) if only the activity of the volatile component is required. Nevertheless, if the volatility of one of the components is much higher than that of the others, the rate of compositional shift can be such that shorter evaporation times are necessary in order to avoid fast distillation. This is not the case for the Al–Cu–Sn system since the volatility of the components is comparable. The IEM was used only to compare the activity data to those yielded by the RKM model since mass loss measurements are time consuming. A further disadvantage of the IEM is that the data obtained from a single evaporation experiment belong only to that particular composition and to the particular temperature of isothermal evaporation, *i.e.*, the initial set-up parameters of the evaporation experiments.

In addition to using the IEM-VDA technique to make vapour pressure measurements over alloys it has also been used to determine the vapour pressure of pure liquid Al since there is a large discrepancy in the literature concerning its vapour pressure data. This is due to the creeping process of the molten Al through the orifice, which contributes to the mass loss caused by vaporisation. Thus the actual 'vapour pressure' obtained from the total mass loss is inaccurate, *i.e.*, it is higher than the true value. In certain systems the surface tension of the liquid sample on the applied cell material is so low that not only the vapour but also the liquid sample flows out through the orifice. This creeping phenomenon maybe unobservable to the naked eye but is noticeable from the enhanced mass loss and from the broader shutter profile. We also experienced this creeping phenomenon for pure liquid Al from the alumina cell, and to a smaller extent on pure liquid Cu from the same cell. This undesirable phenomenon can be restricted by the following: (a) using an alternative cell material, (b) using the same cell material but in a much more porous form to create a larger inner surface area, (c) using an inner liner (cup), as a sample holder, made of porous material or (d) using a channel-type orifice having low Clausing factor. Despite this, instead of choosing most of the above-listed solutions (a, b and d) and making a trial and error experiment, in addition to method c, we decided to determine the vapour pressure over

pure liquid Al using the vapour deposition method. The essence of this solution is that only the mass loss and not the vapour pressure is affected by creeping. We deposited the vapours over pure liquid Al and, in a subsequent experiment, over pure liquid Sn on the same piece of sticky-tape over the same time interval and using the same cell. The layered deposit film of Al and Sn was then dissolved in acid and the concentration ratio of Al to Sn determined by ICP-AOS. We chose tin as a reference substance since liquid Sn does not creep from the alumina cell, and therefore, we consider the literature vapour pressure of liquid Sn to be reliable. The vapour pressure of Al was determined using Eq. (30) which is derived from Eq. (27):

$$\frac{p_{Al}}{p_{Sn}} = \frac{m_{Al}}{m_{Sn}}\sqrt{\frac{M_{Sn}}{M_{Al}}} \tag{30}$$

where m_{Al} and m_{Sn} denote the masses of Al and Sn in the layered deposit film, respectively.

The third method, which is also a conventional KEMS technique, used to determine the activities of Al, Cu and Sn, was the so called Gibbs–Duhem ion intensity ratio (GD-IIR) method, introduced by Belton and Fruehan first for binary and then later for ternary systems [15,17]. This method is also used for comparison purposes since calculations are made only for measured compositions (without interpolation). A study by Bencze et al., who applied this method to the ternary solid Al–Fe–Ni system, is found in Ref. [18]. The activity coefficients of the components in the Al–Cu–Sn system, using the GD-IIR method can be expressed by Eqs. (31)–(33) as follows:

$$\ln\gamma_{Cu}(X) = \ln\gamma_{Cu}(X_{ref}) - \int_{X_{ref}}^{X} X_{Al}\,d\ln\left(\frac{I^+_{Al}X_{Cu}}{I^+_{Cu}X_{Al}}\right) - \int_{X_{ref}}^{X} X_{Sn}\,d\ln\left(\frac{I^+_{Sn}X_{Cu}}{I^+_{Cu}X_{Sn}}\right) \tag{31}$$

$$\ln\gamma_{Sn}(X) = \ln\gamma_{Sn}(X_{ref}) - \int_{X_{ref}}^{X} X_{Cu}\,d\ln\left(\frac{I^+_{Cu}X_{Sn}}{I^+_{Sn}X_{Cu}}\right) - \int_{X_{ref}}^{X} X_{Al}\,d\ln\left(\frac{I^+_{Al}X_{Sn}}{I^+_{Sn}X_{Al}}\right) \tag{32}$$

$$\ln\gamma_{Al}(X) = \ln\gamma_{Al}(X_{ref}) - \int_{X_{ref}}^{X} X_{Cu}\,d\ln\left(\frac{I^+_{Cu}X_{Al}}{I^+_{Al}X_{Cu}}\right) - \int_{X_{ref}}^{X} X_{Sn}\,d\ln\left(\frac{I^+_{Sn}X_{Al}}{I^+_{Al}X_{Sn}}\right) \tag{33}$$

where X_{ref} denotes the mole fraction of the reference alloy at which the Gibbs–Duhem integration starts.

5. Results and discussion

Fig. 1 shows the experimental compositions of Al–Cu–Sn alloys. As can be seen, some compositions were measured twice or more at different times. Thirty-one compositions in the form of 41 samples were studied at eight fixed copper mole fractions, X_{Cu} = 0.10, 0.20, 0.30, 0.333, 0.40, 0.50, 0.60 and 0.70.

As is usual in a KEMS investigations made over a medium temperature range (100–200 K), the logarithm of the measured ion intensity ratio *vs.* the reciprocal of temperature at a fixed composition is a linear function. This means that the enthalpy change of evaporation (or sublimation) is not temperature dependent over this relatively small temperature range. Table 1 gives the *A* ('intercept') and *B* ('slope') parameters of both $\ln[(I^+_{Al}X_{Cu})/(I^+_{Cu}X_{Al})] = A_{AlCu} + B_{AlCu}/T$ and $\ln[(I^+_{Al}X_{Sn})/(I^+_{Sn}X_{Al})] = A_{AlSn} + B_{AlSn}/T$. The slope

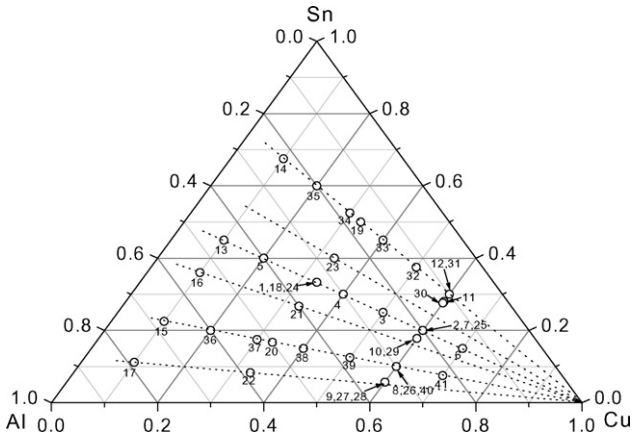

Fig. 1. Composition of the samples measured.

(B_{AlCu}) multiplied by the universal gas constant times −1(i.e. $-R$) represents the difference in the enthalpy changes of evaporation of the two components in the alloy ($\Delta_{vap}H_{Cu} - \Delta_{vap}H_{Al}$). Extracting $\ln[(I^+_{Al}X_{Cu})/(I^+_{Cu}X_{Al})]$ from $\ln[(I^+_{Al}X_{Sn})/(I^+_{Sn}X_{Al})]$, the *A* and *B* parameters of $\ln([(I^+_{Cu}X_{Sn})/(I^+_{Sn}X_{Cu})]) = A_{CuSn} + B_{CuSn}/T$ can be obtained where $A_{CuSn} = A_{AlSn} - A_{AlCu}$ and $B_{CuSn} = B_{AlSn} - B_{AlCu}$. The measured values of $\ln[(I^+_{Al}X_{Cu})/(I^+_{Cu}X_{Al})]$ *vs.* $1/T$ and that of $\ln[(I^+_{Al}X_{Sn})/(I^+_{Sn}X_{Al})]$ *vs.* $1/T$ for selected compositions are plotted in Fig. 2. The measurements were apportioned into two runs, Run 1 and 2, since there was a more than 2-month-long measurement break between the two runs. In principle the effect of time can be significant because after a long time operation of the equipment the mass spectrum may change due to continuous or sudden change in the ion source and multiplier conditions. According to the theory the mass spectrum belonging to the same composition must not change with the time significantly when one applies the RKM-KEMS method for the evaluation of mixing thermodynamic data. Therefore, the RKM-KEMS calculations were performed using both runs individually and using also the complete data-set (uniting Run 1 and 2) in order to study the effect of time and the dimension of the input database on the obtained results.

The liquid binary *L*-parameters, that are necessary for performing the RKM model calculations, were taken from Refs. [8–12]. Table 2 gives a comparison of the binary *L*-data taken from all of these sources while Fig. 3 shows a comparison of the liquid binary G^E data, calculated from all literature sources of binary *L*-data. Clearly, the G^E data of Al-Cu and Al–Sn, obtained from the different sources agree and only Hultgren's [11] G^E data for Al–Cu deviate slightly from those of the other two sources [8,10], whereas, Hultgren's [11] G^E data for the Cu–Sn system significantly deviates from those of Refs. [9,12].

For the next step we had to decide whether to use the data of Run 1 and Run 2 separately or use a merged data-set for obtaining the three ternary *L*-parameters from a multiple regression. Another decision was whether to apply all the three ion intensity ratio methods ('*Al^+/Sn^+ method*', '*Al^+/Cu^+ method*' or '*Cu^+/Sn^+ method*') separately or to select one of them for evaluating the data. Furthermore, we had to decide which of the binary *L*-data-sets, either the consistent COST-data ([8] and [9]) or the alternative databases ([10–12]), to use for calculating the quantities of *Ys* and *Ysummas*.

Using the measured ion intensity ratio (Al^+/Sn^+, Al^+/Cu^+ and Cu^+/Sn^+) data *YYs* (Eqs. (5), (9) and (16)) the binary *Ls* from COST databases (Refs. [8,9]) *Ys* (Eqs. (6b), (10) and (20)) were calculated. It was then possible to calculate *Ysummas* according to Eqs. (4), (8) and (18). In the next step the three ternary *L*-parameters were determined based on Eqs. (3), (7) and (17) by multiple regressions. The latter present *Ysumma vs.* three independent variables as a four-

Table 1
Parameters of $\ln(I^+_{Al}X_{Cu}/I^+_{Cu}X_{Al}) = A_{AlCu} + (B_{AlCu}/T)$ and $\ln(I^+_{Al}X_{Sn}/I^+_{Sn}X_{Al}) = A_{AlSn} + (B_{AlSn}/T)$ equations for all the measured Al–Cu–Sn compositions.

Sample	Date of meas.	Temp. range K	Composition			$\ln(I^+_{Al}X_{Cu}/I^+_{Cu}X_{Al}) = A_{AlCu} + (B_{AlCu}/T)$		$\ln(I^+_{Al}/I^+_{Cu})$ at 1373 K[a]	$\ln(I^+_{Al}X_{Sn}/I^+_{Sn}X_{Al}) = A_{AlSn} + (B_{AlSn}/T)$		$\ln(I^+_{Al}/I^+_{Sn})$ at 1373 K[a]
	mm/dd/yy		X_{Al}	X_{Cu}	X_{Sn}	A_{AlCu}	B_{AlCu}		A_{AlSn}	B_{AlSn}	
1[b]	1/9/07	1273–1453	0.333	0.333	0.333	2.9355	−904.99	9.780	4.8873	−7341.3	0.598
2[b]	1/11/07	1303–1453	0.2	0.6	0.2	4.8843	−5785.1	0.666	6.3982	−11156	0.182
3[b]	1/15/07	1293–1473	0.25	0.5	0.25	4.0844	−3763.6	1.750	6.1720	−10377	0.240
4[b]	1/16/07	1273–1473	0.3	0.4	0.3	1.9430	93.506	5.765	4.4789	−7268.6	0.478
5[b]	1/17/07	1313–1493	0.4	0.2	0.4	3.4077	−790.01	35.636	5.0415	−6901.7	1.058
6[b]	1/19/07	1293–1493	0.15	0.7	0.15	1.1810	−2780	0.094	3.1550	−7799.2	0.078
7[b]	2/1/07	1273–1453	0.2	0.6	0.2	2.2296	−2473	0.512	3.4471	−7627.5	0.121
8[b]	2/6/07	1273–1473	0.3	0.6	0.1	2.1135	−1813.4	1.254	3.8602	−8741.4	0.272
9[b]	2/13/07	1273–1473	0.343	0.6	0.057	1.9434	−1268.5	1.598	3.0044	−7745.7	0.467
10[b]	2/14/07	1273–1473	0.222	0.6	0.178	1.6176	−2042.9	0.432	3.2057	−7344.7	0.152
11[b]	2/16/07	1273–1473	0.12	0.6	0.28	2.0702	−1996.6	0.374	3.7430	−6927.9	0.118
12[b]	2/19/07	1273–1473	0.1	0.6	0.3	3.5293	−4441.6	0.230	5.4293	−9366.7	0.092
13[b]	2/20/07	1273–1473	0.45	0.1	0.45	3.1826	−56.638	98.92	2.7063	−3247.2	1.361
14[b]	2/21/07	1273–1473	0.225	0.1	0.675	2.4286	496.48	37.600	3.2186	−3373.6	0.740
15[b]	2/22/07	1273–1473	0.675	0.1	0.225	3.1774	863.74	297.771	3.5747	−4864.6	3.117
16[b]	2/23/07	1273–1473	0.54	0.1	0.36	2.6699	1138.8	179.533	3.4396	−4269	2.070
17[b]	3/6/07	1273–1473	0.788	0.1	0.112	1.5841	3040.1	352.518	2.8600	−4620.86	4.441
18[b,c]	3/7/07	1273–1473	0.333	0.333	0.333	2.7505	−199.98	13.636	3.9100	−5899.4	0.672
19[b,c]	3/8/07	1273–1473	0.167	0.333	0.5	4.3462	−3159.6	4.000	4.3650	−6186.4	0.312
20[b,c]	3/9/07	1273–1473	0.5	0.333	0.167	2.1161	1287.3	30.980	3.4850	−5865.6	1.344
21[b,c]	3/12/07	1273–1473	0.4	0.333	0.267	2.4010	457.6	18.121	3.5103	−5463.5	0.879
22[b,c]	3/13/07	1273–1473	0.583	0.333	0.083	2.3737	1434.6	50.909	4.3370	−7440.4	2.383
23[b,c]	3/14/07	1273–1473	0.267	0.333	0.4	2.1987	174.38	17.475	3.9000	−5496.3	0.896
24[c]	5/22/07	1273–1453	0.333	0.333	0.333	2.9874	−574.67	12.303	3.9062	−5685.5	0.744
25[c]	5/23/07	1273–1473	0.2	0.6	0.2	2.4732	−2496.3	0.636	3.9100	−7814.7	0.169
26[c]	5/24/07	1273–1473	0.3	0.6	0.1	2.8345	−2449.2	1.464	5.1107	−9996.2	0.361
27[c]	5/30/07	1373–1473	0.343	0.6	0.057	2.9007	−2359	1.918	4.9395	−9831.7	0.676
28[c]	6/1/07	1273–1473	0.343	0.6	0.057	2.0698	−1144.8	2.000	4.7332	−9962.8	0.486
29[c]	6/4/07	1313–1473	0.222	0.6	0.178	2.5842	−2405.4	0.868	4.1659	−8383.3	0.203
30[c]	6/6/07	1313–1473	0.124	0.6	0.276	2.1054	−2274.9	0.322	5.5236	−9843.8	0.087
31[c]	6/7/07	1333–1473	0.1	0.6	0.3	1.7482	−1923.5	0.258	4.0394	−7625	0.108
32[c]	6/12/07	1313–1473	0.125	0.5	0.375	2.1712	−1618.9	0.672	3.4896	−6268.1	0.118
33[c]	6/13/07	1293–1473	0.15	0.4	0.45	2.8522	−1524.4	2.125	4.1255	−6123.6	0.236
34[c]	6/14/07	1273–1473	0.175	0.3	0.525	3.0663	−1077.3	1.715	4.0492	−5438.2	0.342
35[c]	6/15/07	1293–1473	0.2	0.2	0.6	3.1694	−844	12.438	3.6855	−4495.4	0.494
36[c]	6/19/07	1293–1473	0.6	0.2	0.2	3.0818	833.03	126.214	4.2293	−6240.4	2.241
37[c]	6/20/07	1273–1473	0.525	0.3	0.175	2.0000	1620.6	42.011	3.3672	−5604.6	1.463
38[c]	6/22/07	1293–1473	0.45	0.4	0.15	2.1231	823.78	16.911	3.3211	−6021	1.028
39[c]	6/22/07	1293–1473	0.375	0.5	0.125	1.6640	530.07	5.664	3.8158	−7458.9	0.591
40[c]	6/27/07	1373–1473	0.3	0.6	0.1	1.5964	−596.45	1.610	4.4696	−9125.7	0.325
41[c]	6/27/07	1293–1473	0.225	0.7	0.075	1.8241	−3065	0.220	4.3032	−9478.6	0.225

[a] Original measured (not fitted) ratios.
[b] Measurements of Run 1.
[c] Measurements of Run 2.

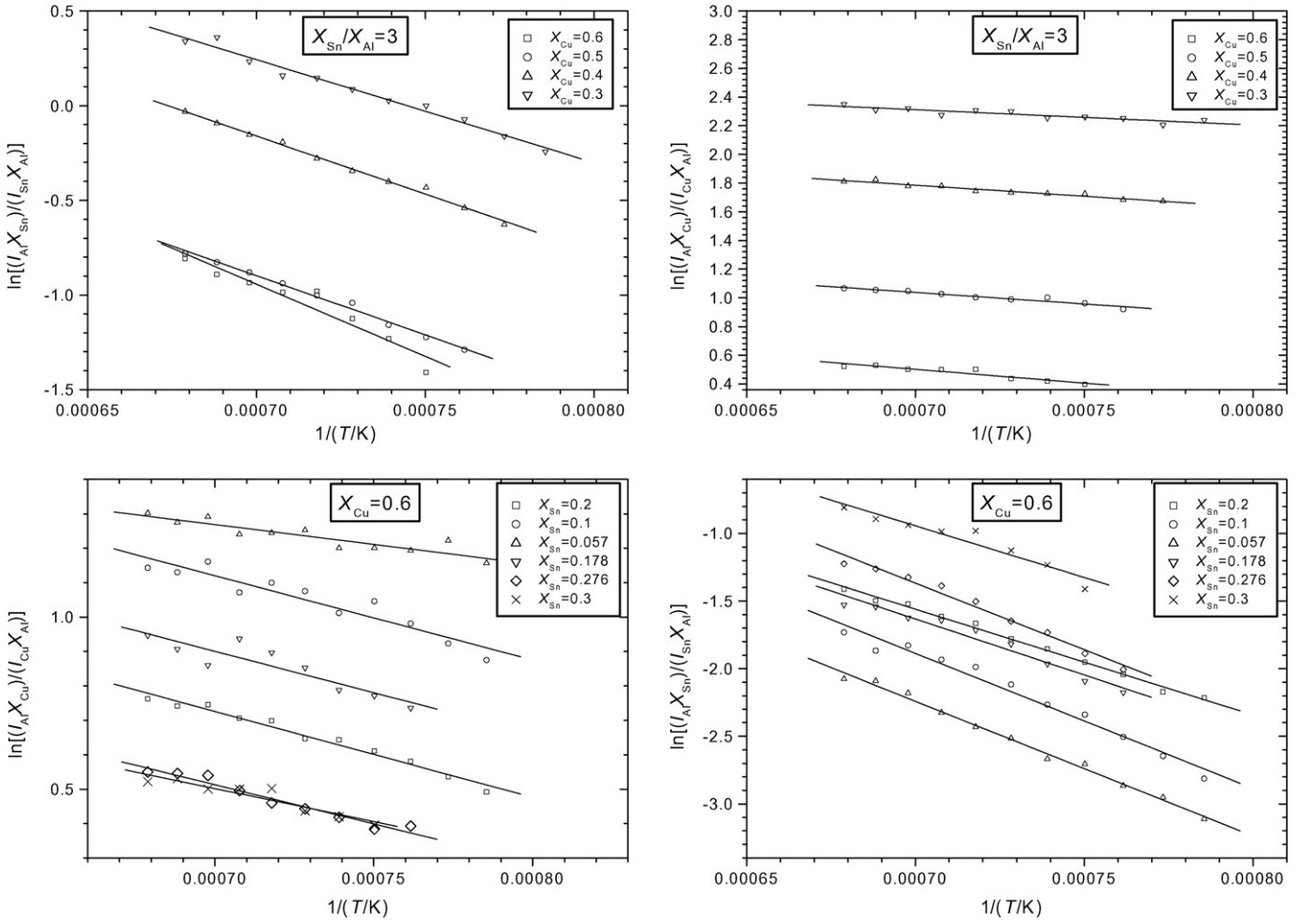

Fig. 2. The measured values of $\ln[(I^+_{Al}X_{Sn})/(I^+_{Sn}X_{Al})]$ *vs.* $1/T$ and that of $\ln[(I^+_{Al}X_{Cu})/(I^+_{Cu}X_{Al})]$ *vs.* $1/T$ for selected compositions.

dimensional function. In order to show the correlation of the data in spite of the four-dimension-difficulty as a graph, in addition to calculating the correlation coefficient of the multi-linear regression, the appropriate two-dimensional functions were also plotted to visualise the regression. Fig. 4 shows the calculated *Ysumma*, *i.e.*, *Ysummacalc*, against *Ysumma* using all 41 measurements (merged data of Run 1 and Run 2) and all three ion intensity ratio methods. The quantity *Ysummacalc* was calculated by multiplying the

Table 2
Comparison of the literature liquid binary *L*-data obtained from Refs. [8–12].

	Hultgren [11]				COST 507 [8]				Witusiewicz et al. [10]			
	A	*B*	*C*	*L* at 1273 K	*A*	*B*	*C*	*L* at 1273 K	*A*	*B*	*C*	*L* at 1273 K
L^0_{AlCu}	−36290	−13.74	0	−53780	−66622	8.1	0	−56310	−67094	8.555	0	−56200
L^1_{AlCu}	146300	7.9	0	24690	46800	−90.8	10	22220	32148	−7.118	0	23090
L^2_{AlCu}	131800	−8.322	0	2589	−2812	0	0	−2812	5915	−5.889	0	−1582
L^3_{AlCu}	−100500	−1.04	0	−11370	0	0	0	0	−8175	6.049	0	−474.623

	Hultgren [11]				COST 507 [8]			
	A	*B*	*C*	*L* at 1273 K	*A*	*B*	*C*	*L* at 1273 K
L^0_{AlSn}	16160	−4.854	0	9981	16329.85	−4.98306	0	9986
L^1_{AlSn}	3227	−0.372	0	2753	4111.97	−1.15145	0	2646
L^2_{AlSn}	2885	−2.302	0	−45.446	1765.43	−0.5739	0	1035
L^3_{AlSn}	1633	−1.167	0	147.409	0	0	0	0

	Hultgren [11]				COST 531 [9]				Miettinen [12]			
	A	*B*	*C*	*L* at 1273 K	*A*	*B*	*C*	*L* at 1273 K	*A*	*B*	*C*	*L* at 1273 K
L^0_{CuSn}	−9821	−7.8	0	−19750	−9002.8	−5.8381	0	−16430	−8124	−6.553	0	−16470
L^1_{CuSn}	−20110	1.94	0	−17640	−20100.4	3.6366	0	−15470	−23970	7.037	0	−15010
L^2_{CuSn}	−5946	−5.4	0	−12820	−10528.4	0	0	−10530	−25124	13.566	0	−7854
L^3_{CuSn}	−3543	−2.266	0	−6428	0	0	0	0	−10213	10.042	0	2570

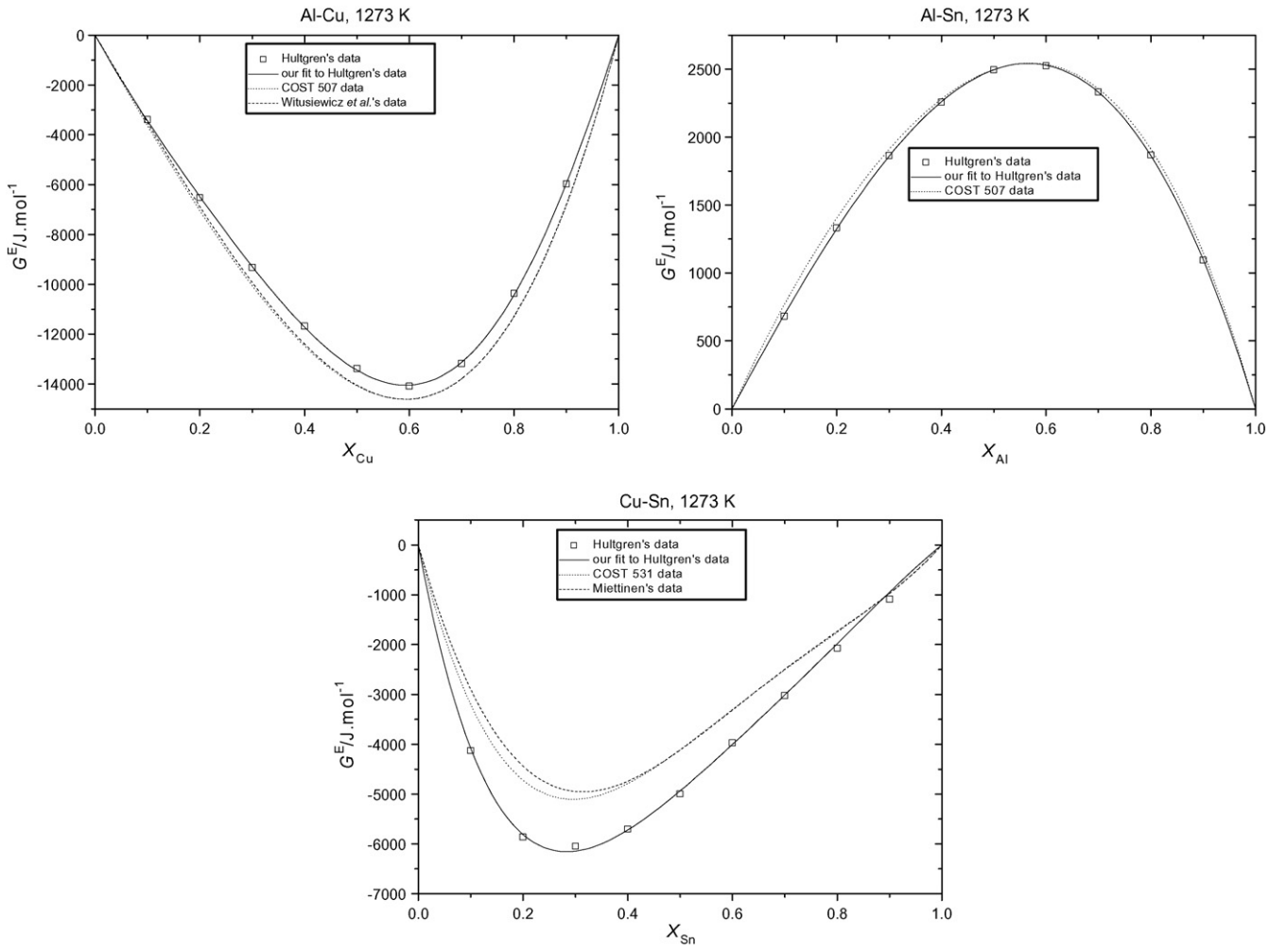

Fig. 3. Excess Gibbs energies of the three boundary liquid binary systems, obtained from Refs. [8–12].

ternary *L*-parameters obtained from the multi-linear regression, with the three independent variables including the mole fractions according to Eqs. (3), (7) and (17). In case of zero statistical and systematic errors, the intercept and the slope of this function should be 0 and 1, respectively. Therefore, these parameters, together with the correlation coefficient of the multi-linear regression can characterise the uncertainty and the reliability of the obtained ternary *L*-parameters. The intercept and the slope data obtained using the 'Cu^+/Sn^+ method' deviate only slightly from ideal and the scatter is low. In contrast, the corresponding values obtained using the 'Al^+/Sn^+ and Al^+/Cu^+ methods' are weaker and more scattered. This is probably due to the auto-ionisation of Al and therefore the data obtained from the 'Cu^+/Sn^+ method' were accepted as being reliable. Although the ternary *L*-data obtained from the 'Al^+/Sn^+ and Al^+/Cu^+ methods' are similar to those obtained using the 'Cu^+/Sn^+ method' their uncertainties are larger.

Table 3 gives the ternary *L*-parameters, obtained using the 'Cu^+/Sn^+ method', at five temperatures in the measurement temperature range (1273–1473 K) for Run 1 and Run 2 and at two extrapolated temperatures (800 and 1000 K) for the merged run. It is not surprising that by increasing the number of regression points the uncertainties of the obtained ternary *L*s decrease and therefore the lowest uncertainties can be obtained for the values of the merged run (all 41 points). Clearly, certainly the data obtained from the merged run must be the most reliable, whereas the *L*-data obtained from Run 1 (23 points) are similar to those obtained from the merged run (41 points). The data obtained from Run 2 (24 points) are further away. The temperature dependence of the ternary *L*s was fitted to a general form of $A + BT + CT\ln(T)$ by regression using only the values of the measurement temperature range. The fitted functions were then extrapolated to 800 and 1000 K. Fig. 5 shows an extrapolation only for the merged run and compares these functions to the ones of Miettinen [12]. Fig. 5 also shows how the extrapolated *L*-values coincide with the individual values obtained directly from the KEMS-RKM regression for the same temperatures. This indicates that the individual *L*-values must be reliable even at 800 and 1000 K in spite of their higher uncertainties. At 800 and 1000 K the obtained *L*-values possess higher uncertainties since they are far from the measurement temperature range. Fig. 5 also shows that Miettinen's [12] *L*-data significantly deviate from our own values. And that whereas the two $L^{(0)}_{AlCuSn}$ data agree well, the agreement of the corresponding $L^{(2)}_{AlCuSn}$ data is poorer and the two $L^{(1)}_{AlCuSn}$ data disagree. This can be attributed to the fact that Miettinen's [12] assessment is valid only at the Cu-rich corner of the Al–Cu–Sn system. In contrast, we took our measurements and made the KEMS-RKM calculations over a large compositional range.

The ternary *L*s, obtained in this work from the data of Run 1, Run 2 and the merged run also differ to some extent but plotting the data of ternary interaction part of G^E at 1273 K (Fig. 6), obtained from the different runs results-in surprisingly very small differences. These differences are also small over the complete measured temperature range (1273–1473 K). We present only the ternary interaction part in the expression of G^E (see Eq. (2)) since the binary parts arise from

Table 3
Ternary L-parameters obtained by the multi-linear regression at five or seven selected temperatures using the binary L-databases from Refs. [8] and [9] and using the ion intensity ratios measured in this work for Run 1, Run 2 and also for the merged run. A, B and C are parameters of the $L(T)$ functions.

T/K	Obtained in this work using the 'Cu^+/Sn^+ *method*' and merging the data of Run 1 and 2 (41 measurements)				Data of Miettinen [12]		
	$-C_{CuSn}$ (intercept)	L^0	L^1	L^2	L^0	L^1	L^2
800	−12170 ± 750	31520 ± 32040	143900 ± 20220	56250 ± 29530	30000	−66000	90000
1000	−11170 ± 560	33130 ± 23610	139700 ± 14900	47630 ± 21760	30000	−76000	90000
1273	−9769 ± 340	34620 ± 14380	133300 ± 9080	34850 ± 13260	30000	−89650	90000
1323	−9510 ± 320	34820 ± 13420	132000 ± 8470	32410 ± 12370	30000	−92150	90000
1373	−9249 ± 300	35000 ± 12840	130700 ± 8100	29930 ± 11840	30000	−94650	90000
1423	−8988 ± 300	35150 ± 12700	129400 ± 8020	27430 ± 11710	30000	−97150	90000
1473	−8726 ± 310	35290 ± 13050	128000 ± 8230	24900 ± 12030	30000	−99650	90000
	$-C_{CuSn} = -(15760 \pm 132) + (1.34 \pm 0.79)T + (0.471 \pm 0.096)T\ln(T)$				$L^0 = 30000$		
	$L^0 = (14270 \pm 1270) + (100.1 \pm 7.6)T - (11.77 \pm 0.93)T\ln(T)$				$L^1 = -26000 - 50T$		
	$L^1 = (145600 \pm 9780) + (101.6 \pm 58.7)T - (15.56 \pm 7.14)T\ln(T)$				$L^2 = 90000$		
	$L^2 = (76730 \pm 1240) + (79.2 \pm 7.4)T - (15.69 \pm 0.91)T\ln(T)$						

T/K	Obtained in this work using the 'Cu^+/Sn^+ *method*' from the data of Run 1 (23 compositions)				Obtained in this work using the 'Cu^+/Sn^+ *method*' from the data of Run 2 (24 compositions)			
	$-C_{CuSn}$ (intercept)	L^0	L^1	L^2	$-C_{CuSn}$ (intercept)	L^0	L^1	L^2
1273	−9305 ± 350	38780 ± 14020	129800 ± 10720	34610 ± 12880	−11320 ± 670	−6900 ± 19270	151000 ± 10710	17880 ± 22390
1323	−9096 ± 350	36870 ± 13850	131800 ± 10590	32400 ± 12720	−10930 ± 610	−833.9 ± 17550	145500 ± 9760	16730 ± 20400
1373	−8886 ± 360	34930 ± 14150	133800 ± 10820	30140 ± 13000	−10540 ± 560	5265 ± 16330	139900 ± 9080	15560 ± 18980
1423	−8676 ± 370	32980 ± 14890	135800 ± 11380	27860 ± 13680	−10140 ± 540	11390 ± 15680	134200 ± 8720	14370 ± 18230
1473	−8465 ± 400	30990 ± 16020	137800 ± 12250	25550 ± 14720	−9747 ± 540	17550 ± 15720	128500 ± 8740	13160 ± 18270
	$-C_{CuSn} = -14220 + 1.622\,T + 0.313T\ln(T)$				$-C_{CuSn} = -19610 - 2.504\,T + 1.262T\ln(T)$			
	$L^0 = 70140 + 70.534\,T - 13.311T\ln(T)$				$L^0 = -139600 - 15.615T + 16.763T\ln(T)$			
	$L^1 = 78880 + 40T + (6.167\mathrm{E}{-8})T\ln(T)$				$L^1 = 240600 + 210.586T - 39.298T\ln(T)$			
	$L^2 = 68680 + 96.66T - 17.264T\ln(T)$				$L^2 = 32910 + 66.63T - 10.972T\ln(T)$			

The numbers behind ± represent standard deviations.

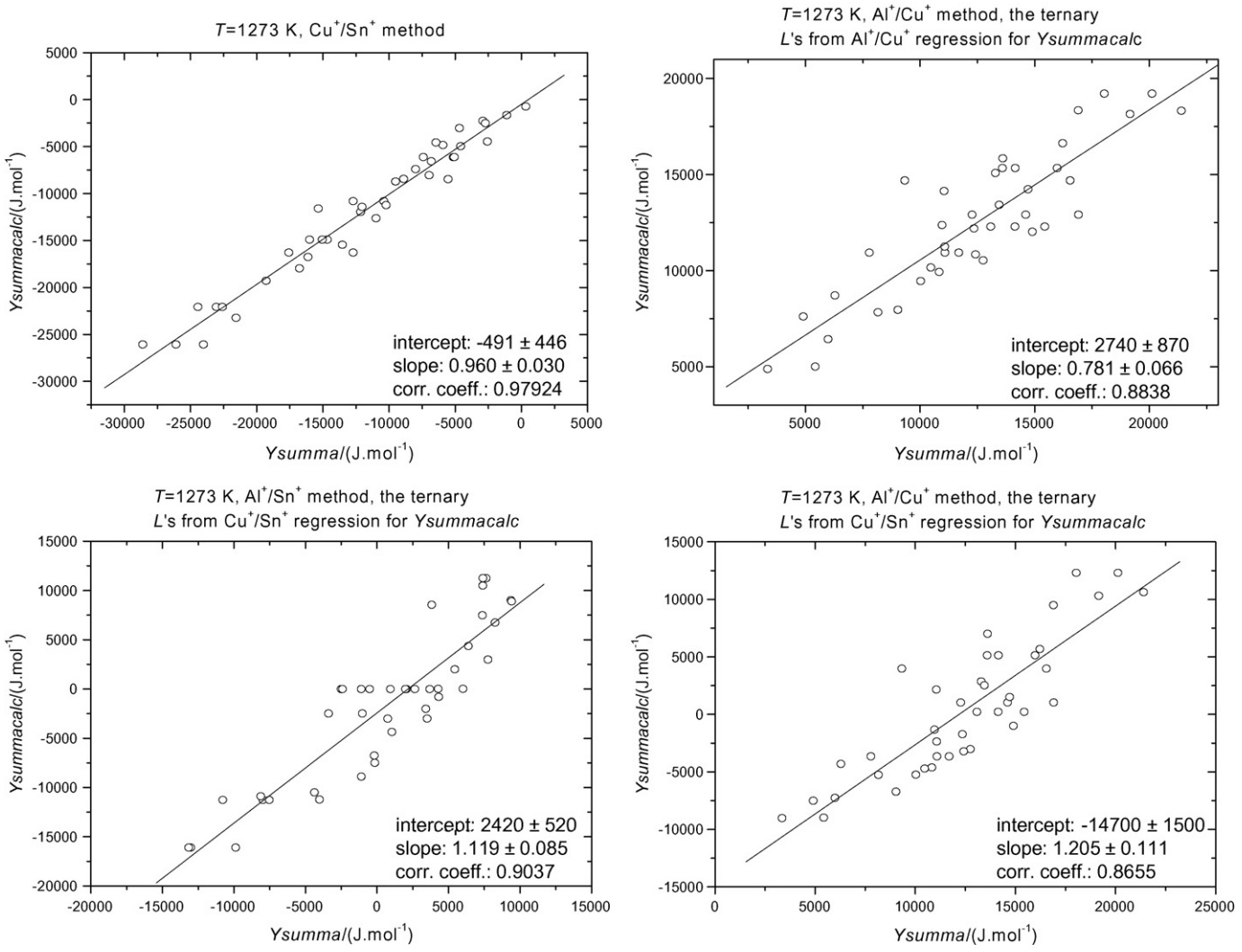

Fig. 4. *Ysummacalc* as a function of *Ysumma* using all the 41 measurements (merged data of Run 1 and Run 2) and using all the three ion intensity ratio methods ('*Al⁺/Sn⁺, Al⁺/Cu⁺ and Cu⁺/Sn⁺ methods*') at 1273 K.

the literature and their values are relatively larger. For the activity values, negligible differences are apparent also among the different runs (Fig. 7). In spite of their being good reproducibility of activities and G^E in the different runs, due to the poorer reproducibility of ternary *Ls*, for phase diagram calculations we recommend using only the ternary *L*-data obtained from the combined 41 measurements ('merged run') since they have the lowest uncertainties. The recommended ternary *Ls*, obtained from the merged (combined) run using the '*Cu⁺/Sn⁺* method', are as follows:

$$L^{(0)} = (14270 \pm 1270) + (100.1 \pm 7.6)T - (11.77 \pm 0.93)T\ln(T) \quad (34)$$

$$L^{(1)} = (145600 \pm 9780) + (101.6 \pm 58.7)T - (15.56 \pm 7.14)T\ln(T) \quad (35)$$

$$L^{(2)} = (76730 \pm 1240) + (79.2 \pm 7.4)T - (15.69 \pm 0.91)T\ln(T) \quad (36)$$

Nevertheless, the activity of Sn, obtained from these ternary *L*-data belonging to the merged run is slightly anomalous at around 1273 K for certain compositions since this temperature is probably near to the liquidus temperatures of those compositions. Therefore, in Fig. 7, we presented the comparison of the iso-activity plots, obtained from the different runs at high temperature (1453 K). As for a_{Sn}, Run 2 estimates more reliable data at around 1273 K.

To confirm the reliability of the RKM activity data, the data in Table 4 were compared to that provided by the IEM using Eqs. (26)–(28). Table 4 shows that $Al_{1/3}Cu_{1/3}Sn_{1/3}$ and $Al_{0.2}Cu_{0.6}Sn_{0.2}$ were prepared twice whereas $Al_{0.225}Cu_{0.700}Sn_{0.075}$ was prepared only once. During the first preparations of $Al_{1/3}Cu_{1/3}Sn_{1/3}$ and $Al_{0.2}Cu_{0.6}Sn_{0.2}$ the samples were evaporated using a more transparent, knife-edged type cell ($C = 1.00$, ¢ = 0.90 mm) while in the second involved the use of a less transparent, channel-type cell ($C = 0.42$, ¢ = 0.50 mm, $l = 1.4$ mm). The geometric difference of the two cells is reflected in the mass loss rate data. In all cases the sample was evaporated at least twice. Instead of taking a fresh portion we used the residue of the previously evaporated sample. The residues were weighed after terminating the evaporation, cooling the samples and taking them out of the vacuum to yield the total (all-component) mass loss. After weighing the residues at room temperature, they were reloaded back into the Knudsen evaporator and heated up to the evaporating temperature again to start a new subsequent evaporation run. The total mean mass loss rate was calculated not only from the integral (by time) evaporation (called as 'sum') but also from the individual evaporation runs. The activity data were calculated using the integral evaporation only (Table 4). Since the statistical error of the mean mass loss rate, calculated from the individual evaporation rates, is low, the integral

Table 4
Activities of some selected Al–Cu–Sn compositions determined by both IEM-VD and RKM methods at 1453 K in the IEM-VD experiments. The estimated uncertainty in the RKM activity data is below 5%.

Composition	Run	Clausing factor	Orifice diameter mm	Temperature K	Evap. time h	Total mass loss mg	Total mass loss rate mg/h	a_{Al} NAA(ICP-AOS) [RKM]	a_{Cu} NAA(ICP-AOS) [RKM]	a_{Sn} NAA(ICP-AOS) [RKM]
$Al_{0.225}Cu_{0.7}Sn_{0.075}$	a	1.00	0.90	1453	22.63	9.82	0.4339	–		–
$Al_{0.225}Cu_{0.7}Sn_{0.075}$	b	1.00	0.90	1453	21.72	9.86	0.4540	–		–
$Al_{0.225}Cu_{0.7}Sn_{0.075}$	Sum	1.00	0.90	1453	44.35	19.68	0.4437	0.0285 (0.0189)	0.449 (0.458)	0.154 (0.155)
	Mean						0.4440 ± 0.0143	[RKM:0.029]	[RKM:0.358]	[RKM:0.156]
$Al_{0.2}Cu_{0.6}Sn_{0.2}$	a	0.42	0.50	1453	65.00	4.61	0.0709			
$Al_{0.2}Cu_{0.6}Sn_{0.2}$	b	0.42	0.50	1453	67.27	5.12	0.0761			
$Al_{0.2}Cu_{0.6}Sn_{0.2}$	Sum	0.42	0.50	1453	132.27	9.73	0.0736	0.0305 (0.0368)	0.229 (0.263)	0.347 (0.331)
	Mean						0.0735 ± 0.0037	[RKM:0.054]	[RKM:0.250]	[RKM:0.353]
$Al_{0.2}Cu_{0.6}Sn_{0.2}$	a	1.00	0.90	1453	19.05	12.25	0.6430	–		–
$Al_{0.2}Cu_{0.6}Sn_{0.2}$	b	1.00	0.90	1453	20.62	13.06	0.6335	–		–
$Al_{0.2}Cu_{0.6}Sn_{0.2}$	Sum	1.00	0.90	1453	39.67	25.31	0.6381	0.0414 (0.0384)	0.285 (0.302)	0.375 (0.369)
	Mean						0.6383 ± 0.0068	[RKM:0.054]	[RKM:0.250]	[RKM:0.353]
$Al_{1/3}Cu_{1/3}Sn_{1/3}$	a	0.42	0.50	1453	23.00	2.46	0.1070	–		–
$Al_{1/3}Cu_{1/3}Sn_{1/3}$	b	0.42	0.50	1453	24.25	2.41	0.0994	–		–
$Al_{1/3}Cu_{1/3}Sn_{1/3}$	c	0.42	0.50	1453	26.83	2.26	0.0842	–		–
$Al_{1/3}Cu_{1/3}Sn_{1/3}$	d	0.42	0.50	1453	46.27	4.21	0.0910			
$Al_{1/3}Cu_{1/3}Sn_{1/3}$	Sum	0.42	0.50	1453	120.35	11.34	0.0942	0.110	0.110	0.488
	Mean						0.0954 ± 0.0099	[RKM:0.232]	[RKM:0.087]	[RKM:0.574]
$Al_{1/3}Cu_{1/3}Sn_{1/3}$	a	1.00	0.90	1453	13.08	12.21	0.9332			
$Al_{1/3}Cu_{1/3}Sn_{1/3}$	b	1.00	0.90	1453	10.97	10.28	0.9374			
$Al_{1/3}Cu_{1/3}Sn_{1/3}$	c	1.00	0.90	1453	12.00	11.21	0.9342			
$Al_{1/3}Cu_{1/3}Sn_{1/3}$	Sum	1.00	0.90	1453	36.05	33.70	0.9348	0.179 (0.203)	0.096 (0.102)	0.629 (0.614)
	Mean						0.9349 ± 0.0022	[RKM:0.232]	[RKM:0.087]	[RKM:0.574]

The activity data, obtained using the analytical data of ICP-AOS, are in parentheses whereas the values obtained using NAA stand in front of the parentheses. The IEM activities were obtained using the vapour pressures of the pure components obtained in this work (*see* the data in bold in Table 7). The corresponding data provided by the RKM method are in square brackets for comparison.

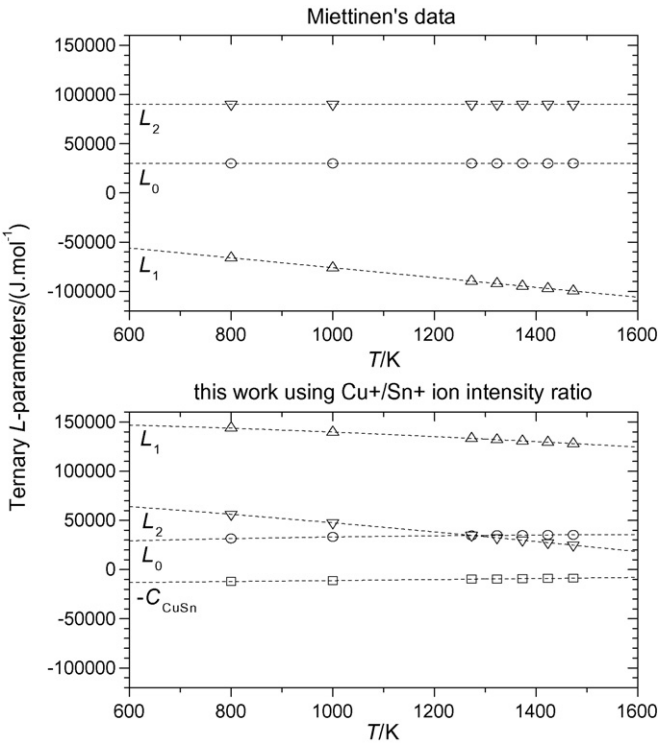

Fig. 5. Bottom: the RKM ternary *L*-parameters as a function of temperature obtained from the merged run using the '*Cu⁺/Sn⁺ method*'. Top: the same parameters assessed by Miettinen [12].

mass loss rate is close to the mean mass loss rate. This means that it is sufficient to calculate the activities from the integral mass loss rate only. Since the individual mass loss rate data are very close to each other, *i.e.*, the statistical error is low, there is no significant compositional shift caused even during the integral evaporation.

The vapour deposits were first analysed by NAA and then using ICP-AOS (Table 5). The activity data, obtained using the analytical data from the ICP-AOS, are in parentheses whereas the values obtained using NAA stand in front of the parentheses. Both datasets are combined with the same integral-total mass loss rate. The vapour deposit data provided by NAA and ICP-AOS differ slightly but in the case of ICP-AOS data the deposit composition deviation and the activity deviation between the two preparations of the same alloy sample (*e.g.*, $Al_{1/3}Cu_{1/3}Sn_{1/3}$) is lower. This means that the uncertainties of the data of the ICP-AOS measurements must also be lower. This is probably due to the ICP-AOS providing the same concentration uncertainties for all the three components (not selective), whereas, using NAA, the uncertainty associated with the Al-concentrations is higher than that associated with the other components.

Since Eqs. (26) and (27) provide only the partial pressures, in order to obtain the activities of the components, Eqs. (28) or (29) must be applied, *i.e.*, the vapour pressures over the liquid pure components at the same temperature are required. To obtain these vapour pressures two possibilities exist: (i) to obtain the data from the literature or (ii) to determine them in-house. Since there are sufficiently large differences for the same vapour pressure quoted by different literature sources, we decided to determine them ourselves. Table 6 shows vapour pressure measurements determined

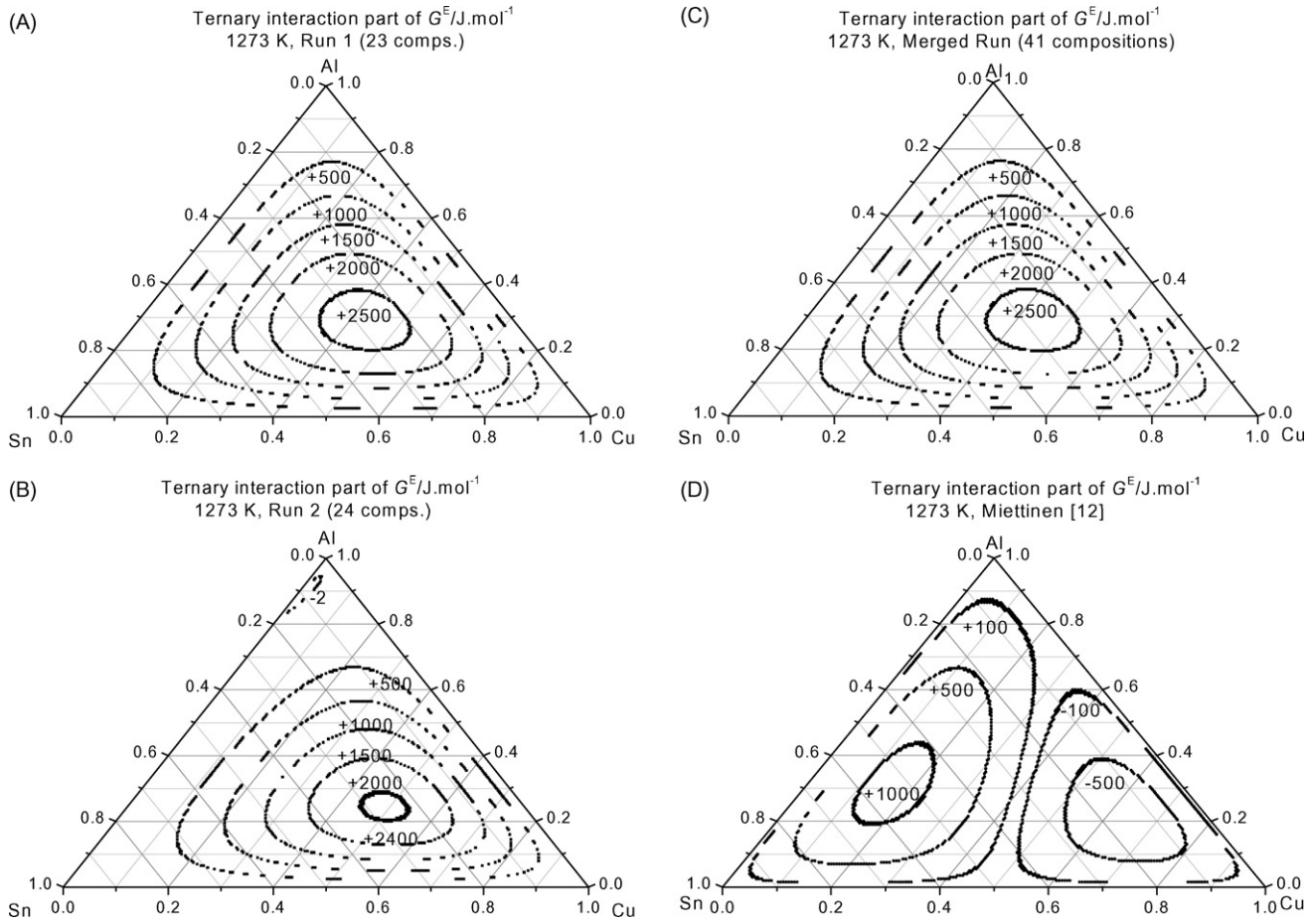

Fig. 6. The iso-curves of the ternary interaction part of excess Gibbs energy at 1273 K, obtained from Run 1 (A), Run 2 (B) and the merged run (C) using the '*Cu⁺/Sn⁺ method*', and from Miettinen' s [12] data (D), using literature binary *L*-parameters from [8,9].

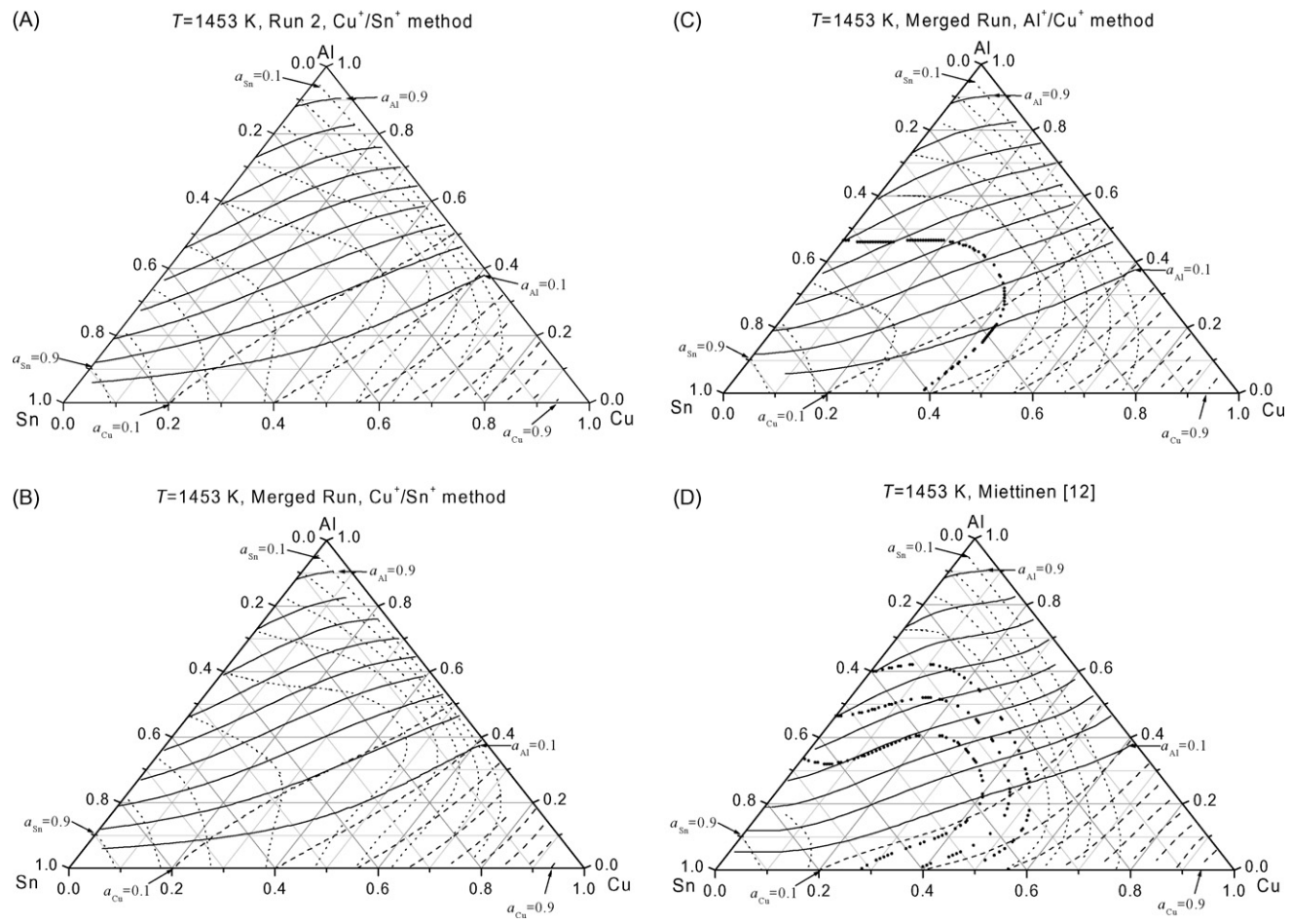

Fig. 7. The iso-activity curves at 1453 K, obtained from Run 2 (A) and the merged run (B) using the *Cu⁺/Sn⁺ method*, from the merged run using the *Al⁺/Cu⁺ method* (C), and from Miettinen' s [12] data (D), using literature binary *L*-parameters from [8,9].

in our laboratory while Table 7 also includes the vapour pressures from various literature sources for comparison. In Table 7 the discrepancy is particularly large concerning Al, less so concerning Cu and negligible in the case of Sn. The reason for this scatter is the different degree of the liquid creeping, enhancing the mass loss and affecting the pressure data. This difference is most likely due to the different interior geometry, porosity and quality of the Knudsen cells used during the literature investigations based on the mass loss technique. Since we observed liquid creeping of Al from our alumina cells, particularly when using knife-edged cells ($C = 1$, ¢ = 0.90 mm) we can conclude that alumina is not the optimal cell material to prevent the creeping of Al. In addition, we were able to observe the creeping of liquid Cu from the alumina cells but to a much smaller extent. Creeping of Sn was negligible a fact similar to that reported in the literature. Similarly to Sn, we have never yet to observe any signs of creeping of the liquid Al–Cu–Sn alloy samples. In addition, in accordance with the literature, we observe no creeping of pure liquid Ag from the same cells albeit Ag is not a component of the ternary alloy samples. We used Ag only to determine the transmission factor (Clausing factor (C)) of the cells used for the IEM investigations. Since our experiments with liquid Ag yielded C-data close to the theoretical values of both kinds of cells used in our investigations ($C = 1.00$ and $C = 0.42$) the lack of creeping could be confirmed. Since creeping enhances mass loss, the vapour

Table 5
Analysis of the vapour deposit films using NAA and ICP-AOS.

	J8392 $Al_{0.225}Cu_{0.700}0Sn_{0.075}$		J8393 $Al_{0.2}Cu_{0.6}Sn_{0.2}$		J8394 $Al_{1/3}Cu_{1/3}Sn_{1/3}$		J8045 $Al_{0.2}Cu_{0.6}Sn_{0.2}$	
	Mass mg	Mass ratio	Mass mg	Mass ratio	Mass mg	Mass ratio	Mass mg	Mass ratio
NAA								
Al	1325	0.093	2176	0.055	7482	0.142	1340	0.044
Cu	17923	1.254	12810	0.325	3455	0.066	8548	0.284
Sn[a]	14291	1.000	39424	1.000	52582	1.000	30130	1.000
ICP-AOS								
Al	0.05	0.061	0.105	0.052	0.648	0.165	0.062	0.055
Cu	1.04	1.273	0.71	0.351	0.28	0.071	0.38	0.339
Sn[a]	0.817	1.000	2.02	1.000	3.92	1.000	1.12	1.000

[a] Reference element for the mass ratio.

Table 6
Isothermal evaporation experiments on the liquid pure components at 1453 K.

Sample	Run	Clausing factor	Orifice diameter mm	Temperature K	Evap. time h	Mass loss mg	Mass loss rate mg/h	Pressure Pa
Cu	a	0.42	0.50	1453	49.45	3.74	0.0756	0.2785
Cu	b	0.42	0.50	1453	111.05	7.68	0.0692	0.2547
Cu	c	0.42	0.50	1453	45.67	2.76	0.0604	0.2226
Cu	Sum	0.42	0.50	1453	206.17	14.18	0.0688	0.2533
	Mean						0.0684 ± 0.0076	0.252 ± 0.028
Sn	a	0.42	0.50	1453	20.97	3.36	0.1603	0.4293
Sn	b	0.42	0.50	1453	21.75	3.20	0.1471	0.3942
Sn	c	0.42	0.50	1453	22.65	3.35	0.1479	0.3962
Sn	d	0.42	0.50	1453	23.50	4.34	0.1847	0.4948
Sn	e	0.42	0.50	1453	21.62	3.50	0.1619	0.4338
Sn	Sum	0.42	0.50	1453	110.48	17.75	0.1607	0.4304
	Mean						0.160 ± 0.015	0.430 ± 0.041
Sn	a	1.00	0.90	1453	22.63	28.09	1.2411	0.4310
Sn	b	1.00	0.90	1453	11.00	14.79	1.3445	0.4669
Sn	c	1.00	0.90	1453	11.00	15.83	1.4391	0.4998
Sn	d	1.00	0.90	1453	11.00	16.53	1.5027	0.5219
Sn	e	1.00	0.90	1453	11.00	14.32	1.3018	0.4521
Sn	Sum	1.00	0.90	1453	66.63	89.56	1.3441	0.4668
	Mean						1.366 ± 0.105	0.474 ± 0.037
Cu	a	1.00	0.90	1453	11.00	11.12	1.0109	0.4826
Cu	b	1.00	0.90	1453	11.00	11.01	1.0009	0.4778
Cu	c	1.00	0.90	1453	11.00	9.77	0.8882	0.4240
Cu	d	1.00	0.90	1453	11.00	11.04	1.0036	0.4791
Cu	Sum	1.00	0.90	1453	44.00	42.94	0.9759	0.4659
	Mean						0.976 ± 0.059	0.466 ± 0.028
Al	a	1.00	0.90	1453	11.00	11.69	1.0627	0.7781
Al	b	1.00	0.90	1453	11.00	12.83	1.1664	0.8539
Al	c	1.00	0.90	1453	11.00	11.54	1.0491	0.7681
Al	d	1.00	0.90	1453	11.00	11.99	1.0900	0.7980
Al	Sum	1.00	0.90	1453	44.00	48.05	1.0920	0.7995
	Mean						1.092 ± 0.052	0.800 ± 0.038

pressure obtained from the enhanced mass loss is not accurate, *i.e.*, higher than the true value. Thus, the lowest values in Table 7 are the closest to the true values. The only reliable Al-pressure values, obtained in this work, are those values we obtained using the deposition technique (Eq. (30)) and those from the mass loss using an inner perpendicularly orientated alumina cup within the alumina Knudsen cell. They are the minimal values shown in Table 7. Since our deposition technique, is unaffected by creeping, this technique should provide true vapour pressure data over pure liquid elements. The alternative method, using an inner cup, increases the inner surface area of the cell, and hence, either prevents or reduces creeping. We obtained the IEM-VD activity data in Table 4 using the minimal vapour pressure data of the pure liquid components (marked in bold: Table 7).

Activities were not calculated using the IEM-KEMS method (*see* Eq. (25)). Instead, the ionisation cross-section ratios were calculated using the pressures determined by the IEM-VD technique and by applying Eq. (25) on the different TD ($\ln(IT)$ *vs.* $1/T$) runs of $Al_{1/3}Cu_{1/3}Sn_{1/3}$ and $Al_{0.2}Cu_{0.6}Sn_{0.2}$ (*see* Table 8). As discussed above (*see* Table 4) the IEM-VD experiments involve only three compositions ($Al_{1/3}Cu_{1/3}Sn_{1/3}$ and $Al_{0.2}Cu_{0.6}Sn_{0.2}$ and $Al_{0.225}Cu_{0.700}Sn_{0.075}$) and several TD runs were made at these compositions. Table 8 shows how large the scatter of the σ_{Al}/σ_{Sn} ionisation cross-section ratio for each run is (~20%), whereas the scatter of σ_{Cu}/σ_{Sn} is low (~9%). Therefore, the large scatter of σ_{Al}/σ_{Sn} can be attributed exclusively to the property of Al^+ and it is logical to accept the ternary *L*-parameters arising only from the Cu^+/Sn^+ ion intensity ratio data. In addition, it is possible to obtain the ionisation cross-

Table 7
Vapour pressures of the liquid pure components obtained from the raw data in Table 6 and compared to literature sources.

Source	*C*	p^*_{Ag}/Pa at 1223 K	p^*_{Ag}/Pa at 1273 K	p^*_{Al}/Pa at 1453 K	p^*_{Cu}/Pa at 1453 K	p^*_{Sn}/Pa at 1453 K
IVTANTHERMO (Windows) [21]	–	0.2787	0.7897	0.5808	0.3521	0.5346
IVTANTHERMO (DOS) [22]	–	0.2787	0.7896	0.573	0.359	0.529
CRC Handbook [23,24]	–	–	–	0.577	0.362	0.521
[25–27]	–	–	–	2.286	0.272	1.184
MBE-Komponenten [28]	–	0.2620	0.7702	0.7066	0.3418	0.4539
This work (from the mass loss using a simple cell having a channel-type orifice)	0.42	–	0.7634	–	**0.252 ± 0.028**	**0.430 ± 0.041**
This work (from the mass loss using a simple cell with knife-edged orifice)	1.00	0.277 ± 0.016	–	0.800 ± 0.038	0.466 ± 0.028	0.474 ± 0.037
This work (from the mass loss using a simple cell but including an inner cup (in a perpendicular position) inside the cell, that contains the sample directly)	0.93	–	–	**0.450**	–	–
This work (from vapour deposit)	1.00	–	–	**0.451**[a]	–	–

[a] Using $p^*_{Sn} = 0.430$ Pa (this work) as a reference value in Eq. (30).

Table 8
Ionisation cross-section ratios calculated from different TD ($\ln(IT)$ vs. $1/T$) runs of $Al_{1/3}Cu_{1/3}Sn_{1/3}$ and $Al_{0.2}Cu_{0.6}Sn_{0.2}$ using the vapour pressures determined by IEM-VD.

Composition	Date of TD run	Code of the deposited film									
		J 8045				J 8393					
		Using ICP-AOS data		Using NAA data		Using ICP-AOS data		Using NAA data			
		σ_{Al}/σ_{Sn}	σ_{Cu}/σ_{Sn}	σ_{Al}/σ_{Sn}	σ_{Cu}/σ_{Sn}	σ_{Al}/σ_{Sn}	σ_{Cu}/σ_{Sn}	σ_{Al}/σ_{Sn}	σ_{Cu}/σ_{Sn}		
$Al_{0.20}Cu_{0.60}Sn_{0.20}$	11.1.2007a	0.790	0.351	0.983	0.420	0.841	0.339	0.792	0.367		
$Al_{0.20}Cu_{0.60}Sn_{0.20}$	11.1.2007b	0.698	0.356	0.869	0.426	0.744	0.344	0.700	0.372		
$Al_{0.20}Cu_{0.60}Sn_{0.20}$	1.2.2007a	0.468	0.300	0.583	0.359	0.499	0.290	0.470	0.313		
$Al_{0.20}Cu_{0.60}Sn_{0.20}$	1.2.2007b	0.539	0.293	0.671	0.351	0.574	0.283	0.540	0.306		
$Al_{0.20}Cu_{0.60}Sn_{0.20}$	23.5.2007	0.654	0.334	0.815	0.400	0.697	0.323	0.656	0.349		
$Al_{0.20}Cu_{0.60}Sn_{0.20}$	Mean	0.630 ± 0.128 (20%)	0.327 ± 0.029 (9%)	0.784 ± 0.159 (20%)	0.391 ± 0.035 (9%)	0.671 ± 0.136 (20%)		0.316 ± 0.028 (9%)		0.632 ± 0.128 (20%)	0.341 ± 0.030 (9%)
Composition	Date (TD run)	Code of the deposited film									
		–				J 8394					
		Using ICP-AOS data		Using NAA data		Using ICP-AOS data		Using NAA data			
		σ_{Al}/σ_{Sn}	σ_{Cu}/σ_{Sn}	σ_{Al}/σ_{Sn}	σ_{Cu}/σ_{Sn}	σ_{Al}/σ_{Sn}	σ_{Cu}/σ_{Sn}	σ_{Al}/σ_{Sn}	σ_{Cu}/σ_{Sn}		
$Al_{1/3}Cu_{1/3}Sn_{1/33}$	9.1.2007	–	–	1.081	0.331	0.738	0.452	0.857	0.489		
$Al_{1/3}Cu_{1/3}Sn_{1/33}$	7.3.2007	–	–	1.199	0.227	0.819	0.310	0.951	0.335		
$Al_{1/3}Cu_{1/3}Sn_{1/33}$	22.5.2007	–	–	1.383	0.271	0.944	0.370	1.097	0.400		
$Al_{1/3}Cu_{1/3}Sn_{1/33}$	Mean	–	–	1.221 ± 0.152 (13%)	0.276 ± 0.052 (19%)	0.834 ± 0.104 (13%)		0.377 ± 0.071 (19%)		0.968 ± 0.121 (13%)	0.408 ± 0.077 (19%)

section ratios from the RKM-KEMS regression. As Refs. [4–6] show the intercept ($-C_{CuSn}$) of the multi-linear regression relates to the cross-sectional ratio (σ_{Cu}/σ_{Sn}) as follows:

$$C_{CuSn} = -RT\ln\left(\frac{p^*_{Cu}}{p^*_{Sn}}\right) + RT\ln\left(\frac{\sigma_{Sn}}{\sigma_{Cu}}\frac{\eta_{Sn}}{\eta_{Cu}}\right)$$
$$= \Delta_{vap}G^\circ_{Cu} - \Delta_{vap}G^o_{Sn} + RT\ln\left(\frac{\sigma_{Sn}}{\sigma_{Cu}}\frac{\eta_{Sn}}{\eta_{Cu}}\right) \quad (37)$$

where $\Delta_{vap}G^\circ$ denotes the standard Gibbs energy of evaporation of pure components. The advantage of the latter method is that it belongs to all compositions included in the RKM regression whereas the value obtained from a TD run belongs only to that particular run and requires a vapour pressure ratio, *e.g.*, from the IEM-VD experiments. In order to obtain the cross-section ratio from RKM-KEMS the only additional data required are the standard Gibbs energies of evaporation of the pure liquid metals ($\Delta_{vap}G^\circ$) which we can obtain either from the literature or from our own source. The mean σ_{Cu}/σ_{Sn} value, obtained from the RKM-KEMS regression from 5 temperatures (1273, 1323, 1373, 1423 and 1473 K) taken from the 1273 to 1473 K measured temperature range, is 0.366 ± 0.022 taking the $\Delta_{vap}G^\circ$ data of pure liquid Cu and Sn from Ref. [21]. The low uncertainty value indicates a small drift with temperature. The same quantity, using the same literature source ([21]) as for the $\Delta_{vap}G^\circ$ data, at the temperature of the isothermal evaporation experiments (1453 K) is 0.349. Replacing the $\Delta_{vap}G^\circ$ data of Ref. [21] with our own data obtained for the pure metals from our IEM and IEM-VD experiments at 1453 K the latter value becomes 0.392. The σ_{Cu}/σ_{Sn} values obtained from the combination of the individual TD runs with the IEM-VD data (see Table 8) are close to the values obtained by RKM-KEMS method. The corresponding literature theoretical value (based on Bell et al.'s [19] or Lennon et al.' s [20] equation) at the same electron energy (30 eV) for σ_{Cu}/σ_{Sn} is 0.517. Nevertheless, the scatter of the literature cross-section data is a frequent phenomenon, *i.e.*, the mass spectra provided by different mass spectrometers can differ due to the different mass discrimination effects in the ion source and the detector. Therefore, the measured cross-sections are usually apparent cross-sections. This is not a problem but when determining vapour pressures and activities by means of cross-sections the local apparent cross-sections provided by the home apparatus have to be used in the calculations.

Table 9 and Fig. 8 include a comparison of the RKM activity data with the data obtained using the Gibbs–Duhem (GD) integration based on Eqs. (31)–(33). The selected reference compositions are usually in the middle of the composition range of the integration and the activities belonging to the reference compositions were those obtained by the RKM method. The integration was performed using the raw ion intensity ratio data. The present GD-IIR data are not therefore, entirely independent of modelling, they just show a consistency between the different sources of data. Table 9 and Fig. 8 present an excellent agreement between the GD-IIR and RKM data proving that the RKM model must be valid.

6. Reliability of measurements and sources of errors

The ternary interaction parameters were obtained using the RKM model, the literature binary *L*-parameters and our own KEMS measurements. The KEMS measurements are, in the study of this system, relative, *i.e.*, the ratio of two ion intensities was measured as a function of temperature and composition. There was no need for pressure calibration when making the KEMS measurements in connection with the RKM model, and, therefore no systematic errors originating from the erroneous determination of the instrumental sensitivity appear in the values of activities and the thermodynamic quantities. The main systematic error in the KEMS-RKM thermo-

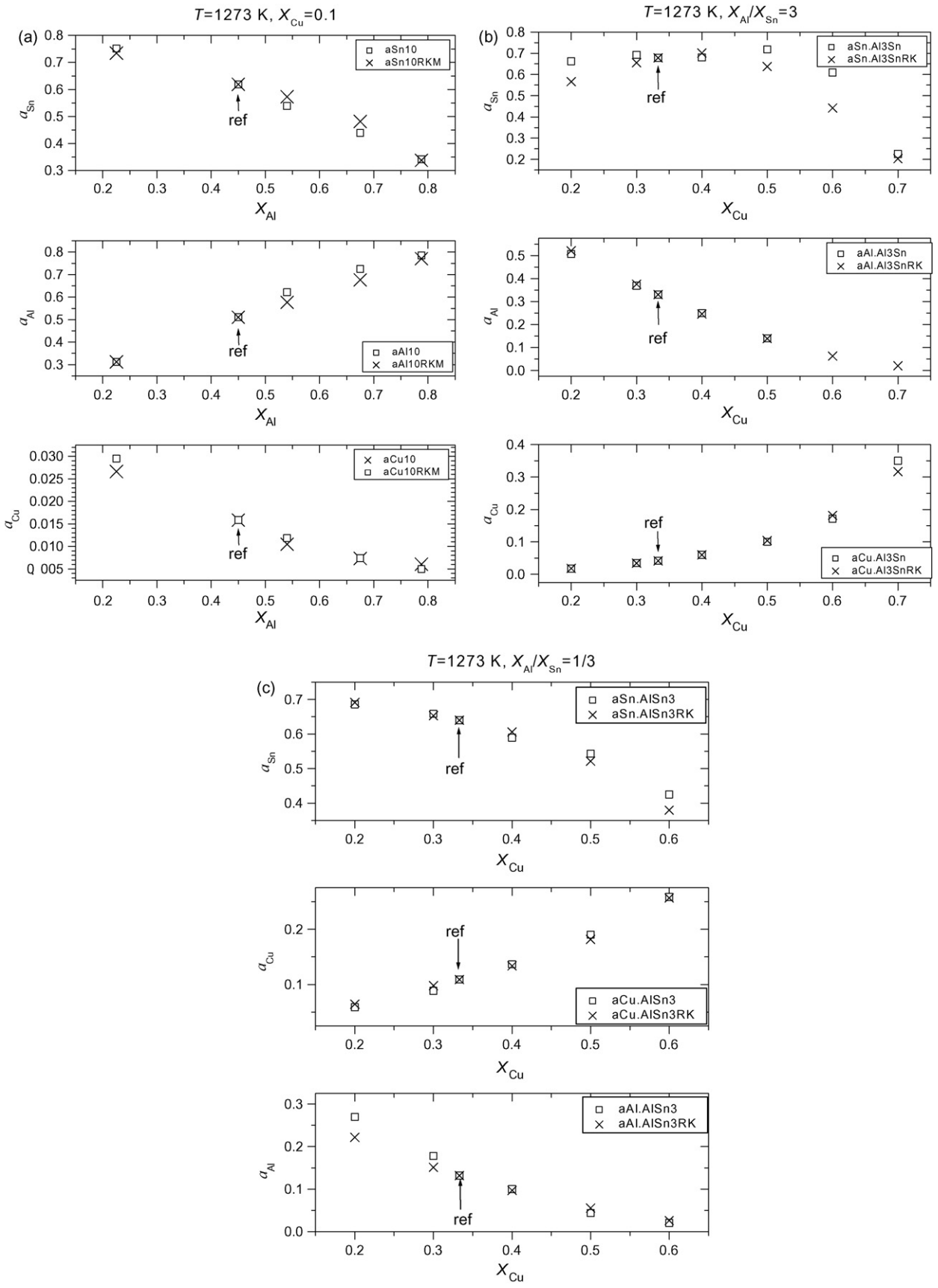

Fig. 8. The activities of certain compositions determined by the GD-IIR method and compared to the data obtained by the RKM method at 1273 K at three isopleths (a: $X_{Cu} = 0.1$, b: $X_{Al}/X_{Sn} = 3$, c: $X_{Al}/X_{Sn} = 1/3$).

Table 9
Activities of certain compositions determined by GD-IIR and compared to the data obtained by the RKM method at 1273 K. Estimated uncertainty of the RKM activity data is below 5%.

Composition	RKM model using 'Cu$^+$/Sn$^+$ method' and merged run			GD-IIR		
	a_{Al}	a_{Cu}	a_{Sn}	a_{Al}	a_{Cu}	a_{Sn}
$X_{Cu} = 0.1$						
$Al_{0.225}Cu_{0.10}Sn_{0.675}$	0.3125	0.0295	0.7348	0.3119	0.0266	0.7510
$Al_{0.45}Cu_{0.10}Sn_{0.45}$	**0.5106**	**0.0158**	**0.6193**	**0.5106**	**0.0158**	**0.6193**
$Al_{0.54}Cu_{0.10}Sn_{0.36}$	0.5774	0.0118	0.5730	0.6217	0.0105	0.5388
$Al_{0.675}Cu_{0.10}Sn_{0.225}$	0.6765	0.0074	0.4817	0.7259	0.0073	0.4387
$Al_{0.788}Cu_{0.10}Sn_{0.112}$	0.7707	0.0050	0.3376	0.7849	0.0060	0.3414
$X_{Al}/X_{Sn} = 3$						
$Al_{0.6}Cu_{0.2}Sn_{0.2}$	0.5208	0.0184	0.5665	0.5065	0.0173	0.6620
$Al_{0.525}Cu_{0.3}Sn_{0.175}$	0.3754	0.0344	0.6554	0.3688	0.0344	0.6927
$Al_{0.500}Cu_{0.333}Sn_{0.167}$	**0.3304**	**0.0415**	**0.6786**	**0.3304**	**0.0415**	**0.6786**
$Al_{0.45}Cu_{0.4}Sn_{0.15}$	0.2459	0.0600	0.7010	0.2494	0.0598	0.6802
$Al_{0.375}Cu_{0.5}Sn_{0.125}$	0.1389	0.1039	0.6376	0.1396	0.1001	0.7185
$Al_{0.3}Cu_{0.6}Sn_{0.1}$	0.0627	0.1818	0.4421	0.0614	0.1713	0.6091
$Al_{0.225}Cu_{0.7}Sn_{0.075}$	0.0203	0.3168	0.2032	0.0146	0.3499	0.2251
$X_{Al}/X_{Sn} = 1/3$						
$Al_{0.2}Cu_{0.2}Sn_{0.6}$	0.2217	0.0644	0.6910	0.2697	0.0589	0.6855
$Al_{0.175}Cu_{0.300}Sn_{0.525}$	0.1511	0.0980	0.6531	0.1777	0.0886	0.6584
$Al_{0.167}Cu_{0.333}Sn_{0.500}$	**0.1318**	**0.1091**	**0.6397**	**0.1318**	**0.1091**	**0.6397**
$Al_{0.15}Cu_{0.40}Sn_{0.45}$	0.0970	0.1337	0.6057	0.1002	0.1367	0.5892
$Al_{0.125}Cu_{0.500}Sn_{0.375}$	0.0555	0.1816	0.5210	0.0436	0.1901	0.5429
$Al_{0.1}Cu_{0.6}Sn_{0.3}$	0.0259	0.2566	0.3795	0.0204	0.2582	0.4247

Reference compositions for the GD-integration, are in bold.

dynamic data may arise from the literature binary *L*-parameters and from the model itself. It is therefore important to use true (assessed, generally accepted) binary *L*-data. The assessed binary *L*-parameters in Refs. [8,9] proved to be the most reliable data. Another source of error (mainly statistical) concerning the ternary *L*-parameters originates from an insufficient number of compositions, which the deviating ternary *L*-values, obtained from the different runs reflect. Despite this, the uncertainties of the ternary *L*-parameters propagate only to a small extent into the values of the activities and excess Gibbs energy. Nevertheless, for phase diagram calculations, we recommend the use of the ternary *L*-parameters obtained by the merged run.

7. Conclusions

In conclusion we fitted the KEMS data to the RKM model and derived a mathematical procedure for all the three ion-pair variation (Al$^+$/Sn$^+$, Al$^+$/Cu$^+$ and Cu$^+$/Sn$^+$) in order to determine the three ternary *L*-parameters. The resultant thermodynamic data confirm both these mathematical derivations and the consistency of the measurements.

The thermodynamic data obtained using the 'Cu$^+$/Sn$^+$ method' was found to have the lowest uncertainties since the intensity of Al$^+$ is probably scattered due to its additional formation by auto-ionisation.

The reliability of the ternary thermodynamic data, obtained by fitting the KEMS data to the RKM model is dependent on the number of the measured compositions and on the quality of the input binary *L*-data used. The binary *L*-data, obtained from Refs. [8,9] proved to be more realistic than those taken from alternative sources of data.

In particular, the literature vapour pressure of pure liquid Al must deviate significantly (~10–30%) from the true data.

The obtained RKM activities and excess Gibbs energies are in good agreement with the data obtained using an independent KEMS method (IEM-VD) and a semi-independent KEMS method (GD-IIR). Therefore, the RKM model seems to be valid for the liquid Al–Cu–Sn alloy. The excess Gibbs energy and activity data, obtained in this work do not completely agree with the data of Miettinen [12].

Finally, KEMS is a powerful technique for the determination of thermodynamic activities and Gibbs energy of mixing.

Acknowledgements

The financial support of Slovenian Research Agency is gratefully acknowledged. This work is a contribution to the European COST MP0602 Action on "Advanced Solder Materials for High Temperature Application (HISOLD)". Laszlo Bencze wishes to thank for the COST-support to short-term scientific mission trips (STSM) in the framework of this action. The English correction made by Mr. David Heath is also gratefully acknowledged.

References

[1] H.L. Lukas, J. Weiss, E.-T. Henig, Calphad (1982) 229–251.
[2] D.W. Marquardt, J. Soc. Ind. Appl. Math. 11 (1963) 431–441.
[3] E. Königsberger, Calphad 15 (1991) 69–78.
[4] T. Miki, N. Ogawa, T. Nagasaka, M. Hino, Mater. Trans. 42 (2001) 732–738.
[5] A. Popovic, L. Bencze, Int. J. Mass Spectrom. 257 (2006) 41–49.
[6] L. Bencze, A. Popovic, Int. J. Mass Spectrom. 270 (2008) 139–155.
[7] H. Schmidt, J. Tomiska, J. Alloys Compd. 385 (2004) 126–132.
[8] I. Ansara, A.T. Dinsdale, M.H. Rand (Eds.), Thermochemical Database for Light Metal Alloys, vol. 2, Office for Official Publications of the European Communities, Luxembourg, 1998, ISBN: 92-828-3902-8 or Report No. EUR 18499.
[9] A.T. Dinsdale, A. Watson, A. Kroupa, J. Vřeštál, A. Zemanová, J. Vízdal, Atlas of Phase Diagrams for Lead-Free Soldering, ©COST Office, ISBN: 978-80-86292-28-1 or COST 531 Thermodynamic Database v. 2.0.
[10] V.T. Witusiewicz, U. Hecht, S.G. Fries, S. Rex, J. Alloys Compd. 385 (2004) 133–143.
[11] R.R. Hultgren (ed.), Selected Values of the Thermodynamic Properties of Binary Alloys, © 1973 by the American Society for Metals, Library of Congress Catalog Card Number 73-76588, American Society for Metals, Metals Park, Ohio 44073.
[12] J. Miettinen, Metall. Mater. Trans. A 33 (2002) 1639–1648.
[13] J. Drowart, C. Chatillon, J. Hastie, D. Bonnell, Pure Appl. Chem. 77 (4) (2005) 683–737, IUPAC-Technical Report.
[14] A. Popovic, Int. J. Mass Spectrom. 230 (2003) 99–112.
[15] G.R. Belton, R.J. Fruehan, Metall. Trans. 71 (5) (1967) 1403.
[16] Y.M. Muggianu, M. Gambino, L.P. Bros, J. Chem. Phys. 72 (1975) 85–88.
[17] G.R. Belton, R.J. Fruehan, Metall. Trans. 1 (4) (1970) 781.
[18] L. Bencze, T. Markus, S. Dash, D.D. Raj, D. Kath, W.A. Oates, W. Löser, K. Hilpert, Metall. Mater. Trans. A 237 (2006) 3171–3181.
[19] K.L. Bell, H.B. Gilbody, J.G. Hughes, A.E. Kingston, F.J. Smith, J. Phys. Chem. Ref. Data 12 (1983) 891–916.

[20] M.A. Lennon, K.L. Bell, H.B. Gilbody, J.G. Hughes, A.E. Kingston, M.J. Murray, F.J. Smith, J. Phys. Chem. Ref. Data 17 (1988) 1285–1363.
[21] L.V. Gurvich, V.S. Yungman, G.A. Bergman, I.V. Veitz, A.V. Gusarov, V.S. Iorish, V.Ya. Leonidov, V.A. Medvedev, IVTANTHERMO for Windows, Database on thermodynamic properties of individual substances and related software, © 1992–2000 Glushko Thermocenter of Russian Academy of Sciences.
[22] V.S. Yungman, V.A. Medvedev, I.V. Veits, G.A. Bergman, IVTANTHERMO—A Thermodynamic Database and Software System for the Personal Computer, CRC Press and Begel House, Boca Raton, 1993.
[23] CRC Handbook of Chemistry and Physics, 84th ed. online version, CRC Press, Boca Raton, 2003.
[24] C.B. Alcock, V.P. Itkin, M.K. Horrigan, Properties of the Elements and Inorganic Compounds, Vapour Pressure of Metallic Elements, Can. Met. Q. 23 (1984) 309, Sec. 4.
[25] L. Brewer, The thermodynamic and physical properties of the elements, Report for the Manhattan Project (1946).
[26] A.L. Marshall, R.W. Dornte, F.J. Norton, Am. Chem. Soc. 59 (1937) 1161.
[27] E. Baur, R. Bruner, Hev. Chim. Acta 17 (1934) 958.
[28] Database of © 2003 Dr, Eberl MBE-Komponenten GmbH, at http://www.mbe-components.com.